Journal of Scientific Computing (2026) 106:57
https://doi.org/10.1007/s10915-026-03184-0

General Runge–Kutta TASE Methods for Reaction–Diffusion Problems

Dajana Conte[1] · Juan Ignacio Montijano[2] · Giovanni Pagano[3] · Beatrice Paternoster[1] · Luis Rández[2]

Received: 28 March 2025 / Revised: 8 November 2025 / Accepted: 3 January 2026

Abstract
The class of Time Accurate and highly Stable Explicit Runge–Kutta (RK–TASE) methods has been introduced by Bassenne, Fu and Mani (J. Comput. Phys. 2021) and then extended by Calvo, Montijano and Rández (J. Comput. Phys. 2021), and Aceto, Conte and Pagano (Appl. Numer. Math. 2024), for the efficient solution of stiff initial value problems. With the aim of making RK–TASE methods suitable for the efficient solution of semi–discretized reaction–diffusion Partial Differential Equations (PDEs), in this work we exploit a general formulation of the schemes that allows to reduce both their computational cost and error constants, obtaining also good stability properties for such problems. In particular, a thorough study of the accuracy and stability properties leads to new RK–TASE methods up to order five that are more efficient than existing ones. Several experiments show that the new proposed RK–TASE methods are able to efficiently solve models of PDEs from applications that require integration over long time intervals. Furthermore, they show the better performance of the new RK–TASE compared to other numerical schemes from the scientific literature.

Keywords Runge–Kutta methods · Stable time integration · Stiff differential equations · Reaction–diffusion PDEs · Turing–pattern solution

Mathematics Subject Classification 65L04 · 65L05 · 65L06 · 65L20 · 65M12 · 65M20 · 65M22

✉ Giovanni Pagano
giovanni.pagano5@unina.it

Dajana Conte
dajconte@unisa.it

Juan Ignacio Montijano
monti@unizar.es

Beatrice Paternoster
beapat@unisa.it

Luis Rández
randez@unizar.es

[1] Department of Mathematics, University of Salerno, 84084 Fisciano, Italy

[2] Department of Applied Mathematics, University of Zaragoza, 50009 Zaragoza, Spain

[3] Department of Agricultural Sciences, University of Naples Federico II, 80055 Portici, Italy

Published online: 23 January 2026

1 Introduction

Advection–reaction–diffusion Partial Differential Equations (PDEs) originate from several mathematical models related to real–world applications, among which we mention: vegetation evolution [13, 24]; corrosion of metallic materials [16]; electrodeposition process in batteries [18]; multiphase flows in porous media [25]. The semi–discretization of PDEs gives rise to large and stiff Initial Value Problems (IVPs), for which an efficient numerical solution is necessary. In this manuscript, we focus on the efficient numerical solution of stiff systems of first order IVPs

$$\begin{cases} y'(t) = f(t, y(t)), \quad t \in (t_0, t_{\text{end}}], \quad y,\ f \in \mathbb{R}^d, \\ y(t_0) = y_0, \quad y_0 \in \mathbb{R}^d, \end{cases} \tag{1}$$

arising mainly from the space discretization of reaction–diffusion PDEs. Diffusion and/or reaction terms can therefore introduce the stiff behaviour of the solution of (1). Let us assume f to be sufficiently smooth so that (1) has a unique solution $y = y(t)$.

For the numerical solution of (1), well known methods are the s–stage one–step Runge-Kutta (RK) ones [4]. Depending on the choice of the coefficients, they can be explicit or implicit. Explicit methods are simple to implement and their main computational effort is only given by the evaluation of the vector field at the various stages and integration steps. Many examples of explicit RK methods with different orders have been proposed in the literature but, nevertheless, it is well known that they are not suitable for the solution of (1) if it is stiff. Stiff problems can be addressed with implicit methods (e.g. diagonally implicit methods which are less expensive than fully implicit methods), since they can have good stability properties being thus able to handle stiffness. Among implicit RK methods, there are several families (see e.g Hairer and Wanner [21], Hundsdorfer and Verwer [23]) that have good stability properties, but require to solve at each step a nonlinear system of equations with dimension proportional to d, being d the size of (1). This point severely restricts the application of implicit methods.

To overcome this difficulty, linearly implicit methods have been introduced, which require to solve a fixed and generally small number of linear systems at each step. This is the case of Rosenbrock methods [21, 28], that exploit the Jacobian of the vector field $J = D_y f(t, y)$ at each step. In particular, the linear systems to solve have coefficient matrices of the type $(I - h\alpha J)$, being I the identity, h the time step–size and α a positive coefficient. Rosenbrock methods are similar to diagonally implicit RK methods. However, when for the latter the implicit equations are solved e.g. via the Newton method, the related number of iterations and the convergence are not known a priori. Instead, for Rosenbrock methods the number of linear systems to solve is fixed. To avoid the computation of the Jacobian at each step in Rosenbrock methods, the W–methods [21] have been proposed. They exploit an approximate Jacobian W but usually attain a lower order of convergence than Rosenbrock methods with the same number of stages.

An alternative approach to efficiently deal with stiff problems was introduced by Bassenne *et al.* in [3]. These authors propose to stabilize (1) by considering a linear operator $T_p = T_p(hW) \in \mathcal{L}(\mathbb{R}^d, \mathbb{R}^d)$, referred to as a Time–Accurate and highly Stable Explicit (TASE) operator, where W is an approximation of the Jacobian $D_y f(t, y)$. The operator T_p has to be constructed in such a way that the modified problem

$$\begin{cases} u'(t) = T_p(hW)\ f(t, u(t)), \quad t \in (t_0, t_{\text{end}}], \\ u(t_0) = y_0, \end{cases} \tag{2}$$

can be solved efficiently by an explicit RK method, i.e. in such a way that (2) does not inherit the stability difficulties of (1). Furthermore, T_p has to be constructed in such a way that the exact solution of (2) is an order p approximation of the one of (1), where p is the order of the explicit RK method. In this way, the numerical solution of the problem (2) is an order–p approximation of the exact one of the original IVP (1). Therefore, the main goal is to construct the TASE operator T_p in such a way that (2) overcomes the stability restrictions arising when solving the original stiff system (1), while maintaining the order p of the explicit RK method. Moreover, if possible one can require that the RK–TASE method, i.e. the method resulting from the use of the explicit RK scheme on the modified problem (2), has small error coefficients.

The original TASE operators proposed by Bassenne *et al.* [3] depend on a single positive parameter α, for which optimal choices allow to obtain A–stable or A(θ)–stable RK–TASE methods. In a subsequent paper, Calvo *et al.* [9] proposed a generalization of these TASE operators involving p positive parameters α_j, $j = 1, \ldots, p$, for which optimal choices allow to obtain strongly A–stable or A(θ)–stable, or even L(θ)–stable RK–TASE methods. A further step has been given by Aceto *et al.* in [1] by considering TASE operators where the available parameters α_j can also be complex with Re $\alpha_j > 0$, and in this case the conjugate must also be present. This allows, through an appropriate reformulation of the TASE operators, to continue working in real arithmetic in implementation despite the presence of complex coefficients, and to improve the stability and lower the error coefficients of the RK–TASE methods derived by Bassenne *et al.* [3] and Calvo *et al.* [9]. Since RK–TASE methods are promising and competitive with classical RK methods, Rosenbrock methods, and W–methods, research on them has greatly intensified in recent years: additional operators called singly TASE operators have been proposed [7, 10]; new efficient W–methods have been derived from RK–TASE methods [2, 11, 20]; the stability of RK–TASE methods has been studied in detail assuming W completely arbitrary [12]; TASE operators have been used to stabilize parallelizable explicit two–step peer methods [14, 26].

Novelty and structure of the paper. For the derivation of existing RK–TASE schemes, emphasis has been given on A(θ)–stable methods, with θ equal to or close to 90 degrees, and this typically leads to high error constants. However, as we will see, to efficiently solve problems arising from the discretization in space of reaction–diffusion PDEs, due to the spectrum of the related Jacobian the matrix W can be selected in order to have eigenvalues close to the negative real axis without incurring stability issues, and therefore it is possible to require a smaller θ, with the aim of obtaining significantly lower error constants. Starting from the theory developed by Aceto *et al.* in [1], in this paper we perform a comprehensive study of the accuracy and stability of RK–TASE methods using an alternative formulation of the operator T_p, that leads to a reduction in the computational cost of the schemes. Such a study will allow the derivation of new s–stage RK–TASE methods of order $p = s = 2, 3, 4$ with drastically lower error constants than those of existing RK–TASE methods, and with stability properties which make them very suitable and efficient for semi–discretized reaction–diffusion PDEs. A further novelty of this paper is given by the derivation of a new 5–stage RK–TASE method that can reach order $p = 5$ for some classes of problems. We emphasize that, so far in the scientific literature, RK–TASE methods have been proposed only up to order four. Several experiments conducted on PDEs from applications, such as vegetation evolution in some environments and the electrodeposition process in batteries, that are carachterized by large space domain and require integration over long time intervals in order to show Turing patterns–like solutions, testify the efficiency of the new proposed RK–TASE schemes, and their advantages over other numerical methods in the literature, confirming also the theoretical analyses developed in the paper.

This paper is organized as follows: in Section 2 we recall some existing TASE operators and show the TASE operator we are interested in; in Section 3 we study the stability properties of RK–TASE methods; Section 4 is devoted to the derivation of new RK–TASE methods with good stability and low error coefficient, up to order $p = 5$; in Section 5 we perform several tests that confirm the good efficiency of the new RK–TASE methods; in Section 6 we provide concluding remarks and discuss future research. Furthermore: in the Appendix A we report the implementation of the new RK–TASE methods and discuss their computational cost; in the Appendix B we show the derivation of explicit RK schemes of order $p = 4, 5$ used in the experiments.

2 TASE Operators and General RK–TASE Methods

First of all note that s–stage RK–TASE methods can be directly formulated for (1) as

$$\begin{aligned} y_1 &= y_0 + \sum_{j=1}^{s} b_j \; K_j, \\ K_i &= h \; T_p(hW) \; f\left(t_0 + c_i h, \, y_0 + \sum_{j=1}^{i-1} a_{ij} \; K_j \right), \quad i = 1, 2, \ldots, s, \end{aligned} \tag{3}$$

to compute the solution at $t = t_0 + h$, where a_{ij}, b_i, c_i are the coefficients that define the underlying explicit RK method. In this way, the analysis of the properties of the methods is facilitated, by avoiding going through the modified problem (2). As mentioned in the introduction, if the explicit RK method has order p, and $T_p(hW)$ satisfies

$$T_p(hW) = I + C_p \; (hW)^p + \mathcal{O}(h^{p+1}) = I + \mathcal{O}(h^p), \tag{4}$$

then the RK–TASE method (3) also has order p [20], i.e. the numerical solution y_1 satisfies

$$y_1 - y(t_0 + h) = \mathcal{O}(h^{p+1}).$$

Thus, the consistency of the RK–TASE methods follows from that of the underlying explicit RK method. The coefficient C_p in (4) is proportional to the main error terms of the RK–TASE methods, as proved e.g. in [20]. Therefore, the main objective of the TASE operator T_p is to overcome the stability restrictions on h of the explicit RK method when solving stiff systems, possibly also with a small error constant $|C_p|$.

In the original paper of Bassenne *et al.* [3] such TASE operators were constructed from the following observation: when the problem to solve is linear, i.e. when $f(t, y) = Wy$ in (1), the use of the explicit Euler method combined with the TASE operator $T_1(hW) = (I - h \; W)^{-1} = I + \mathcal{O}(h)$ leads to

$$y_1 = y_0 + h \; (I - hW)^{-1} \; W y_0,$$

and this is equivalent to solve (1) by means of the implicit Euler method, that is a first order implicit scheme suitable for stiff systems. Introducing a positive parameter α, the Bassenne *et al.* operators are thus obtained computing recursively $T_p = T_p(hW; \alpha)$ by

$$T_p(hW; \alpha) = \begin{cases} (I - h\alpha W)^{-1} & \text{if } p = 1, \\ \dfrac{2^{p-1}}{2^{p-1} - 1} T_{p-1}(hW; \alpha/2) - \dfrac{1}{2^{p-1} - 1} T_{p-1}(hW; \alpha) & \text{if } p \geq 2, \end{cases} \tag{5}$$

being W an approximation of the Jacobian $J = D_y f(t, y)$. This positive parameter α is selected to get a good balance between the stability properties of RK–TASE methods and minimum $|C_p|$. In particular, the authors in [3] got A–stable RK–TASE methods of order $p = s = 2$, and A(θ)–stable RK–TASE methods of order $p = s = 3, 4$, with $|C_p|$ of the order of magnitude of 10^0 or 10^1. The definitions of stability are recalled in detail in the next section. Also, Table 1 in Section 4 summarizes the properties of the RK–TASE methods by Bassenne and co–workers.

In a subsequent paper, Calvo *et al.* [9] generalized (5) by considering a family of TASE operators depending on a vector of p positive parameters $\underline{\alpha} = (\alpha_1, \ldots, \alpha_p)^T \in \mathbb{R}^p$, given by

$$T_p(hW; \underline{\alpha}) = \sum_{j=1}^{p} \gamma_j \, (I - h\alpha_j W)^{-1} \quad \text{with} \quad \gamma_j = \left(\frac{1}{\alpha_j}\right)^{p-1} \left(\prod_{k \neq j} \left(\frac{1}{\alpha_j} - \frac{1}{\alpha_k} \right) \right)^{-1}. \tag{6}$$

With γ_j as in (6), these TASE operators satisfy (4) with error constant $C_p = \prod_{j=1}^{p} \alpha_j$. Exploting the freedom given by the new parameters, the authors of [9] derived RK–TASE methods with better stability properties than those in [3]. That is, they got strongly A–stable RK–TASE methods of order $p = s = 2$, L(θ)–stable RK–TASE methods of order $p = s = 3$, and strongly A(θ)–stable RK–TASE methods of order $p = s = 4$. Table 1 in Section 4 summarizes the properties of these methods.

Subsequently, Aceto *et al.* in [1] considered TASE operators of type (6), admitting also the case of complex parameters α_j, with $\mathrm{Re}\, \alpha_j > 0$. Indeed, if α_j is complex but its conjugate also appears, then the TASE operator can be written as

$$T_p(hW) = \pi_p(hW)^{-1} \big(\pi_p(hW) - (hW)^p \big), \tag{7}$$

where

$$\pi_p(z) = \prod_{j=1}^{p} \left(z - \frac{1}{\alpha_j} \right) = z^p - \sigma_1 z^{p-1} + \sigma_2 z^{p-2} + \ldots + (-1)^p \sigma_p \tag{8}$$

is a polynomial of degree p having all real coefficients σ_j. Thus, despite the presence of complex coefficients, it is possible to always work in real arithmetic during implementation. As shown in Table 1 in Section 4, in this way the authors managed to improve the A(θ)–stability angle of existing RK–TASE methods and to slightly lower their error constants, which with T_p as in (7)–(8) has size

$$|C_p| = \frac{1}{|\sigma_p|}. \tag{9}$$

Remark 1 Note that RK–TASE methods (3) with TASE operator T_p as in (5), (6), or (7)–(8), are linearly implicit numerical schemes. In particular, using (5) or (6), they require the solution of $s \cdot p$ linear systems at each time–step (p linear systems for each stage due to form of T_p). Instead, when using (7)–(8), the RK–TASE stages K_i in (3) read

$$\Big(\pi_p(hW) \Big) \, K_i = h \Big(\pi_p(hW) - (hW)^p \Big) \, f\Big(t_0 + c_i h, \, y_0 + \sum_{j=1}^{i-1} a_{ij} K_j \Big), \tag{10}$$

and, therefore, it is necessary the solution of only s linear systems at each time–step; indeed, after computing $p - 1$ matrix products which are required to define $\pi_p(hW)$ in (8), each stage involves just one linear system. In this paper, we are interested in RK–TASE methods

with T_p as in (7)–(8), which from now on we denote by general RK–TASE methods. More details on their implementation and computational cost are given in the Appendix.

As we will see from the analyses conducted in the next sections, by assuming that the W matrix corresponds to the Jacobian $J = D_y f(t, y)$ at each step, we can obtain RK–TASE methods with good stability properties. However, we emphasize that for many problems arising from the spatial semi–discretization of PDEs it is possible to choose W constant throughout the numerical integration without incurring stability issues, as shown in [12] for some particular choices of the free parameters in T_p. Therefore, even though we will perform the stability analysis assuming $W = J$, in the implementation we suitably choose a constant W: for example, for reaction–diffusion PDEs, due to the spectrum of the Jacobian of the corresponding semi–discretized version, it is possible to choose a constant W with eigenvalues close to the negative real axis without incurring stability issues, so that even A(θ)–stable methods can be employed with θ not excessively large. Furthermore, in this way the computational cost of general RK–TASE methods is drastically reduced since, before proceeding with the time integration, we can calculate both the $p-1$ matrix products needed to define $\pi_p(hW)$ and a factorization of LU type for it. Thus, the main computational effort of general RK–TASE lies in the solution of just $2s$ triangular linear systems at each time–step due to (10). For more details about this aspect, consult the Appendix.

3 Stability of General RK–TASE Methods

The aim of this section is to study the linear stability properties of RK–TASE methods as a function of the coefficients of the polynomial $\pi_p(z)$ in (8). Since RK–TASE methods are in fact linearly implicit schemes, we have not considered the analysis of non–linear stability properties, such as B–stability, as no meaningful results are expected in this regard. Nevertheless, as shown in [8], A–stability guarantees stable behaviour of the numerical solutions for semi–linear (non–autonomous) problems where the Jacobian matrix of the vector–field does not vary exponentially with time. Many problems arising from semi–discretization of PDEs fit this requirement. Otherwise, fully implicit methods should be considered.

It is worth noting that, unlike previous studies that consider as free parameters α_j or $1/\alpha_j$ in (6), here we take as free parameters the coefficients σ_j of the polynomial $\pi_p(z)$. In this way, as explained above, with $\sigma_j \in \mathbb{R}$ we can simultaneously cover the case where α_j are real or complex and, furthermore, as we will see, we can study stability by considering the Routh–Hurwitz condition on $\pi_p(-z)$, which allows to simplify the analysis.

The study of the linear stability of a general RK method

$$\begin{aligned} y_1 &= y_0 + \sum_{j=1}^{s} b_j \; K_j, \\ K_i &= h \; f\left(t_0 + c_i h, \, y_0 + \sum_{j=1}^{s} a_{ij} \; K_j \right), \quad i = 1, 2, \ldots, s, \end{aligned} \tag{11}$$

is performed by considering the scalar test equation $y'(t) = \lambda \; y(t)$, where λ is a complex constant. Applying the RK method (11) to compute the solution at $t = t_0 + h$, one gets

$$y_1 = R(z) \; y_0,$$

where $z = h\lambda$ and $R = R(z)$ is the RK stability function, that can be written as

$$R(z) = 1 + z\, b^T (I - z\, A)^{-1}\, e, \tag{12}$$

see e.g. [4], being

$$A = (a_{ij})_{i,j=1}^{s} \in \mathbb{R}^{s\times s}, \quad b = (b_1, \ldots, b_s)^T \in \mathbb{R}^s, \quad e = (1, \ldots, 1)^T \in \mathbb{R}^s. \tag{13}$$

Let us define

$$\mu := |R(\infty)| = \left| \lim_{z\to\infty} R(z) \right|. \tag{14}$$

We mention that if the method (11) has order $p = s \leq 4$ and is explicit, i.e. $a_{ij} = 0$ for $j \geq i$, then the function $R(z)$ in (12) can be equivalently written as

$$R_p(z) = 1 + z + \frac{1}{2!}\, z^2 + \cdots + \frac{1}{p!}\, z^p, \tag{15}$$

see [4]. The stability region of the RK method (11) is defined as the set

$$\mathcal{S} = \{z \in \mathbb{C} :\ |R(z)| \leq 1\}. \tag{16}$$

The RK scheme is said to be A–stable if $\mathcal{S} \supset \{z \in \mathbb{C} :\ \text{Re}\ z \leq 0\}$. Also, the method is called:

- A(θ)–stable if $\mathcal{S} \supset \mathcal{S}(\theta) := \{z \in \mathbb{C} :\ \text{Re}\ z \leq 0 \text{ and } |\arg(-z)| \leq \theta\}$;
- strongly A(θ)–stable if it is A(θ)–stable and $\mu < 1$, with μ defined in (14);
- L(θ)–stable if it is A(θ)–stable and $\mu = 0$.

In the above definitions θ can be zero: in this case we have stability only on the negative real axis. Instead, if $\theta = 90$ degrees, the above definitions are called A–stability (as already mentioned), strong A–stability, L–stability, respectively. Clearly, A(0)–stability is necessary for A(θ)–stability for any $\theta > 0$. Moreover, we emphasize that strong A(θ)–stability or even L(θ)–stability are very useful requests for attenuating oscillating phenomena of the numerical solution due to the presence of very stiff components, see e.g. [9].

It is easy to check that, for RK–TASE methods (3), the stability function $RT_p = RT_p(z)$ is just

$$RT_p(z) = R(z\ T_p(z)),$$

with R as in (12). Also, since the underlying RK method is explicit, if $p = s \leq 4$, due to (15) for RK–TASE methods RT_p can be equivalently expressed as

$$RT_p(z) = 1 + (z\ T_p(z)) + \frac{1}{2!}\, (z\ T_p(z))^2 + \cdots + \frac{1}{p!}\, (z\ T_p(z))^p, \tag{17}$$

see e.g. [9]. From now on, we assume $p = s \leq 4$. This assumption will be removed only when we propose a method with $s = 5$.

Proposition 1 *Consider general RK–TASE methods (3) of order $p = s \leq 4$, with T_p as in (7)–(8). Necessary conditions for their A(θ)–stability and strong A(θ)–stability are, respectively, $|R_p(-\sigma_1)| \leq 1$, i.e. $-\sigma_1 \in \mathcal{S}$, and $|R_p(-\sigma_1)| \leq \mu < 1$, being $R_p(z)$ the stability function (15) of the underlying explicit RK, $\mathcal{S}$ as in (16) and μ as in (14).*

Proof As observed in [9], if a general RK–TASE method is A(θ)–stable, then $|RT_p(\infty)| \leq 1$. Since by hypothesis the general RK–TASE methods have order $p = s \leq 4$, RT_p is as in (17). Note that, due to (7)–(8),

$$\lim_{z\to\infty} z\ T_p(z) = -\sigma_1. \tag{18}$$

By (17) and (18), we then have $|RT_p(\infty)| \leq 1 \iff |R_p(-\sigma_1)| \leq 1$. Doing similar steps, the proof of the necessary condition for RK–TASE strong A(θ)–stability also follows.

Let us recall below the Routh–Hurwitz criterion, which will be useful to determine a necessary condition for the A–stability of general RK–TASE methods.

Proposition 2 Routh–Hurwitz criterion [19, p. 194]. *The roots of the polynomial*

$$q(z) = \tilde{g}_0 z^s + g_0 z^{s-1} + \tilde{g}_1 z^{s-2} + g_1 z^{s-3} + \ldots, \quad \tilde{g}_0 \neq 0, \ \tilde{g}_i, \ g_i \in \mathbb{R},$$

have negative real part if and only if

$$\tilde{g}_0 \Delta_i > 0 \ \ \forall \, odd \, i, \qquad \Delta_i > 0 \ \ \forall \, even \, i, \quad i = 1, \ldots, s,$$

being Δ_i be the determinant of the submatrix obtained by selecting the first i rows and columns of

$$H = \begin{pmatrix} g_0 & g_1 & g_2 & \cdots & g_{s-1} \\ \tilde{g}_0 & \tilde{g}_1 & \tilde{g}_2 & \cdots & \tilde{g}_{s-1} \\ 0 & g_0 & g_1 & \cdots & g_{s-2} \\ 0 & \tilde{g}_0 & \tilde{g}_1 & \cdots & \tilde{g}_{s-2} \\ 0 & 0 & g_0 & \cdots & g_{s-3} \\ \vdots & \vdots & & & \vdots \end{pmatrix}, \quad \tilde{g}_i = 0 \ if \ i > \frac{s}{2}, \quad g_i = 0 \ if \ i > \frac{s-1}{2}.$$

Theorem 1 *Necessary conditions for the A–stability of general RK–TASE methods (3) of order $p = s \leq 4$, with T_p as in (7)–(8), are the following.*

$$\begin{aligned} &Case \ p = 2: \ \sigma_j > 0, \ j = 1, 2. \\ &Case \ p = 3: \ \sigma_j > 0, \ j = 1, 2, 3, \quad and \quad \sigma_1 \sigma_2 - \sigma_3 > 0. \\ &Case \ p = 4: \ \sigma_j > 0, \ j = 1, 2, 3, 4, \quad and \quad \sigma_1 \sigma_2 \sigma_3 - \sigma_3^2 - \sigma_1^2 \sigma_4 > 0. \end{aligned} \tag{19}$$

Proof From (7)–(8), note that the stability function (17) of general RK–TASE methods with order $p = s \leq 4$ reads

$$RT_p(z) = 1 + z \, \frac{(\pi_p(z) - z^p)}{\pi_p(z)} + \frac{1}{2!} \, z^2 \, \frac{(\pi_p(z) - z^p)^2}{\pi_p(z)^2} + \cdots + \frac{1}{p!} \, z^p \, \frac{(\pi_p(z) - z^p)^p}{\pi_p(z)^p}.$$

Therefore, the poles of $RT_p(z)$ are the roots of $\pi_p(z)$. By [4, Th. 351B], a necessary condition for RK A–stability is that the mentioned poles belong to the right half plane. Note that, having $\pi_p(z)$ real coefficients, this necessary condition is equivalent to applying the Routh–Hurwitz criterion in Proposition 2 on $\pi_p(-z)$, $p = 2, 3, 4$. By doing this, the thesis follows.

Remark 2 By [1, Th. 2.2], a necessary condition for A(θ)–stability is:

$$\text{poles of } RT_p(z) \text{ located outside } S(\theta) := \{z \in \mathbb{C} : \ \text{Re } z \leq 0 \text{ and } |\arg(-z)| \leq \theta\}.$$

This is clearly satisfied for arbitrary θ if the poles of $RT_p(z)$ reside in the right half plane. Since the conditions expressed in Theorem 1 have been derived by requiring that these poles are in the right half plane, we will therefore exploit them also in the search for A(θ)–stable methods. Indeed, this procedure also allows to identify necessary conditions for A(θ)–stability that do not imply restrictions on the angle θ.

The conditions in Proposition 1 and Theorem 1 significantly simplify the derivation of the coefficients σ_j of general RK–TASE methods.

4 New General RK–TASE Methods up to Order Five

In this section we construct general RK–TASE methods up to order five with good stability properties and low error coefficients. Unlike previous works, our study will focus not only on A–stable or A(θ)–stable numerical methods with θ as large as possible, but also on methods with extremely low error constant $|C_p|$ (9). Furthermore, we also derive very efficient RK–TASE methods that can reach order $p = 5$, which are not yet present in the literature.

Specifically, each of the following Subsections 4.1–4.4 focuses on constructing a method of different order, through the procedure described below:

- we express the TASE operator of order p by highlighting the free coefficients and the necessary conditions they must satisfy for A–stability;
- we then prove necessary and sufficient conditions on the coefficients to get strong A(θ)–stability and, when possible, L(θ)–stability, which are essential requirements for treating highly stiff problems;
- next, we analyze how the stability angle θ and the error constant $|C_p|$ vary for the possible configurations of the remaining free coefficients;
- finally, we derive the coefficients of a specific method that achieves a good balance between small error constant and sufficiently large stability angle.

As we will see from numerical tests, the new general RK–TASE methods derived here are able to solve without stability issues several PDEs of interest in applications, and with much lower errors than the RK–TASE methods introduced so far in the scientific literature.

4.1 RK–TASE with Order Two

Here we consider a general RK–TASE method with two stages and order two, denoted with RKTASE2, which through (7)–(8) is obtained using the TASE operator $T_2(hW)$ defined by

$$T_2(z) = \frac{\pi_2(z) - z^2}{\pi_2(z)}, \quad \text{with} \quad \pi_2(z) = z^2 - \sigma_1 z + \sigma_2. \tag{20}$$

Using Theorem 1, thus imposing for stability that $\pi_2(-z)$ is a Routh–Hurwitz polynomial, by (19) the real coefficients σ_1 and σ_2 must satisfy

$$\sigma_1 > 0, \quad \sigma_2 > 0. \tag{21}$$

From (17), the stability function of the RKTASE2 method is

$$RT_2(z) = 1 + (z\ T_2(z)) + \frac{1}{2}\ (z\ T_2(z))^2\,, \tag{22}$$

and the stability function $R_2(z)$ of the undelying explicit RK method is given by RT_2 in (22) with $T_2(z) = 1$, see (15).

Through Proposition 1, a necessary condition for A(θ)–stability is $-\sigma_1 \in \mathcal{S}_2$, with

$$\mathcal{S}_2 = \{z \in \mathbb{C} :\ |R_2(z)| \le 1\}, \tag{23}$$

see (16). The region $\mathcal{S}_2$ is represented in the left Figure 1. Since $\sigma_1 \in \mathbb{R}$, we can limit ourselves to considering only the real part of $\mathcal{S}_2$, which is given by the interval $[-2, 0]$. Taking into account (21), we thus consider

$$\sigma_1 \in (0, 2]. \tag{24}$$

When choosing the free coefficients for a method, it is important to consider also strong stability. Let us therefore prove the following result.

Proposition 3 *The function $|RT_2(\infty)|$ attains its minimum value corresponding to 1/2 at $\sigma_1 = 1$, for every σ_2.*

Proof From (18) and (22), note that

$$RT_2(\infty) = 1 - \sigma_1 + \frac{1}{2}\sigma_1^2.$$

Since $RT_2(\infty)$ is positive, we have $|RT_2(\infty)| = RT_2(\infty)$. From the derivative of $RT_2(\infty)$ with respect to σ_1, corresponding to the function $-1 + \sigma_1$, the result follows.

So far, we have worked on the stability in view of the choice of the σ_1 parameter. The following theorem reports the stability conditions also on σ_2 for the RKTASE2 method.

Theorem 2 *The following conditions are necessary and/or sufficient for the A–stability and A(θ)–stability of the RKTASE2 method, respectively.*

1. *The RKTASE2 is A–stable if and only if*

$$(\sigma_1, \sigma_2) \in \Gamma := \left\{(\sigma_1, \sigma_2) \in \mathbb{R}^2;\, \sigma_1 \in (0, 2],\ \sigma_2 \in (0, \sigma_2^*]\right\},$$

where $\sigma_2^* = \sigma_2^*(\sigma_1)$ is the greatest root of the polynomial

$$\rho(\sigma_2) = -4\sigma_1^5 + 16\,\sigma_1^3\sigma_2 + (-16\sigma_1^2 + 4\sigma_1^3)\sigma_2^2 + (8\sigma_1 - 4\sigma_1^2)\sigma_2^3 + (-2 + \sigma_1)\sigma_2^4.$$

2. *The RKTASE2 is A(θ)–stable for some $\theta \geq 0$ if and only if*

$$\sigma_1 \in (0, 2], \quad \textit{and} \quad \sigma_2 \leq \phi(\sigma_1) = (8 - 2\sigma_1) + 4\sqrt{4 - 2\sigma_1}. \tag{25}$$

Proof The first statement follows from [9] and [1]. Indeed, in [9, Th. 2.2] it has been proved that, by considering only real α_j coefficients in (6), RKTASE2 is A–stable for $\sigma_1 \in (0, 2]$ and $\sigma_2 \in (0, \sigma_1^2/4)$, where σ_1 and σ_2 are the coefficients of the polynomial $\pi_2(z)$ in (20), and are linked to α_j in (6) by the relationships $\sigma_1 = 1/\alpha_1 + 1/\alpha_2$ and $\sigma_2 = 1/(\alpha_1\alpha_2)$. Then, in [1, Th. 3.1] it has been proved that, for each pair of positive coefficients (σ_1, σ_2), assuming $\sigma_2 \geq \sigma_1^2/4$, A–stability is obtained when $\sigma_1 \in (0, 2]$ and $\sigma_2 \in [\sigma_1^2/4, \sigma_2^*]$. Combining these two results, the proof of the first statement follows.

The second statement occurs by imposing $|RT_2(z)| \leq 1$ for all real negative z, with $\sigma_1 \in (0, 2]$ from (24).

According to Theorem 2, recalling that the error constant of the general RKTASE2 method is $|C_2| = 1/\sigma_2$ from (9), a good choice could reside in the maximum σ_2 that allows to obtain A–stability, i.e. $\sigma_2 = \sigma_2^*(\sigma_1)$ for any $\sigma_1 \in (0, 2]$. For $\sigma_2 > \sigma_2^*(\sigma_1)$, the RKTASE2 is not A–stable, but can be A(θ)–stable for some θ if (25) is satisfied. Since $\phi(\sigma_1)$ is a monotonic decreasing function of σ_1, its maximum corresponds to $\phi(0) = 16$. Therefore, A(θ)–stable methods for some θ can be obtained only for $\sigma_2 < 16$.

By fixing $\sigma_1 = 1$ for strong stability using Proposition 3, therefore, the choice that guarantees A–stability and minimum error is $\sigma_2 = \sigma_2^*(1) \simeq 1.68125$, for which $|C_2| = 1/\sigma_2 \approx 0.6$. Or, to lower the error constant while still obtaining good stability properties, we can exploit the second statement of Theorem 2, from which we can get A(θ)–stability for some θ by taking $\sigma_2 < \phi(1) = 6 + 4\sqrt{2} \simeq 11.6569$. In order to get low error constant and still relatively large θ, in the numerical experiments we consider the method with $\sigma_2 = 5$. In this way, $|C_2| = 0.2$, and we have strong A(θ)–stability with $\theta = 60.3955$ degrees. The stability region of the method is displayed in the right Figure 1. Finally, for completeness and reader convenience, we report in Figure 2 the value of the A(θ)–stability angle for several choices of the coefficients σ_1 and σ_2. Note that, in accordance with the second statement of Theorem 2, we can get A(θ)–stability only when $\sigma_1 \in (0, 2]$ and $\sigma_2 \leq \phi(\sigma_1)$.

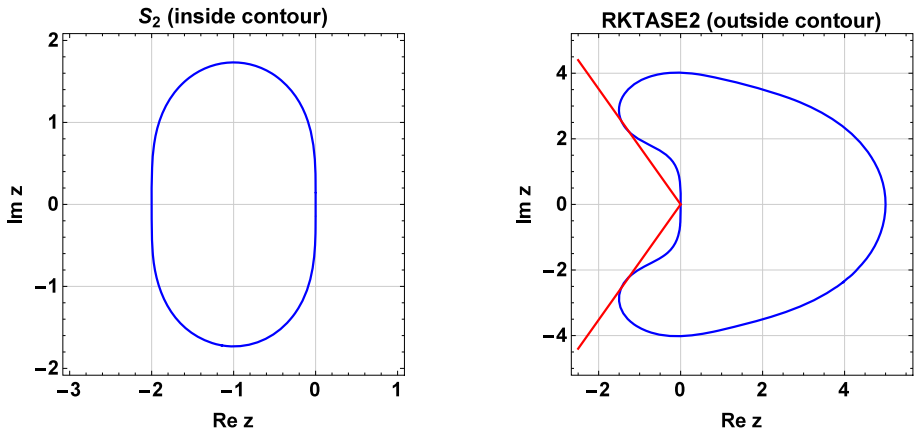

Fig. 1 On the left, region $\mathcal{S}_2$ (23); on the right, stability region of the RKTASE2 method with $\sigma_1 = 1$ and $\sigma_2 = 5$, that is strongly A(θ)–stable with $\theta = 60.3955$ degrees.

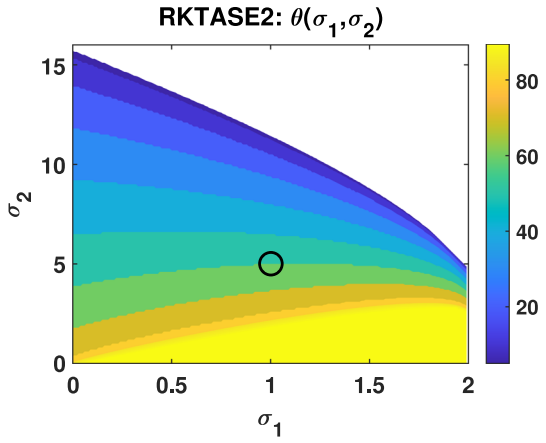

Fig. 2 Angle θ of A(θ)–stability for RKTASE2, by varying σ_1 and σ_2; the symbol 'o' denotes the choice (σ_1, σ_2)=(1, 5) that we made to conduct the numerical tests.

4.2 RK–TASE with Order Three

Here we consider a general RK–TASE method with three stages and order three, denoted with RKTASE3, that in view of (7)–(8) is obtained using the TASE operator $T_3(hW)$ defined by

$$T_3(z) = \frac{\pi_3(z) - z^3}{\pi_3(z)}, \quad \text{with} \quad \pi_3(z) = z^3 - \sigma_1\, z^2 + \sigma_2\, z - \sigma_3.$$

Using (19) from Theorem 1, we consider for stability the following conditions on the real coefficients σ_j:

$$\sigma_1 > 0,\ \sigma_2 > 0,\ \sigma_3 > 0, \quad \text{and} \quad \sigma_1\sigma_2 - \sigma_3 > 0. \tag{26}$$

Recall that by (17) the stability function of the RKTASE3 method is

$$RT_3(z) = 1 + (z\ T_3(z)) + \frac{1}{2}\ (z\ T_3(z))^2 + \frac{1}{6}\ (z\ T_3(z))^3\,. \tag{27}$$

The stability function of the underlying explicit RK method is $R_3(z)$, corresponding to RT_3 in (27) with $T_3(z) = 1$, see (15).

Similarly to the previous subsection, we note that, by Proposition 1, a necessary condition for A(θ)–stability is $-\sigma_1 \in \mathcal{S}_3$, with

$$\mathcal{S}_3 = \{z \in \mathbb{C} : \ |R_3(z)| \leq 1\}, \tag{28}$$

see (16). This leads to

$$\sigma_1 \in (0, z_3], \quad z_3 \simeq 2.51275, \tag{29}$$

see the left Figure 3. To fix σ_1, let us consider the following result.

Proposition 4 *The function $|RT_3(\infty)|$ attains its minimum value corresponding to 0 at $\sigma_1 \simeq 1.59607$, for every $\sigma_2,\ \sigma_3$.*

Proof From (18) and (27),

$$RT_3(\infty) = 1 - \sigma_1 + \frac{1}{2}\,\sigma_1^2 - \frac{1}{6}\,\sigma_1^3.$$

Note that the equation $|RT_3(\infty)| = 0$ admits the real solution $\sigma_1 \simeq 1.59607$, from which the result follows.

From Proposition 4 and (29), we conclude that the choice $\sigma_1 \simeq 1.59607$ is very convenient as it can allow to obtain L(θ)–stability.

Let us then consider the choices of σ_2 and σ_3, for which we have to take into account the conditions in (26). In [9], and also in [1], the authors focus on L(θ)–stable RK–TASE methods with θ as large as possible. In particular, the authors of [1] propose a method with $\theta \simeq 89$ degrees, but characterized by error constant $|C_3| \simeq 6.88379$, and this penalizes its performance. For this reason, here we focus on methods with possibly significantly lower error constants.

After fixing $\sigma_1 = 1.59607$ for L(θ)–stability, we take $\sigma_2 = \sigma_3/\sigma_1 + \epsilon$ in view of (26), being ϵ a small positive constant; in particular, in the following we consider $\epsilon = 10^{-5}$. In this way, the stability function of RKTASE3 depends only on the parameter σ_3. Let us denote it by $RT_3 = RT_3(z; \sigma_3)$. Through a numerical exploration, we have seen that the condition

$$|RT_3(z; \sigma_3)| \leq 1, \quad z \in \mathbb{R}, \quad z \leq 0,$$

holds when $\sigma_3 \leq \sigma_3^* \simeq 20.4$, which is therefore necessary for L(θ)–stability. The right Figure 3 shows the RKTASE3 stability regions for several values of σ_3. In numerical tests, to obtain small error and L(θ)–stability with large enough θ, we choose $\sigma_3 = 10$. By doing so, from (9) the error constant is $|C_3| = 1/\sigma_3 = 0.1$, and the method is L(θ)–stable with $\theta = 50.4281$ degrees.

Also, we report in Figure 4 the value of the L(θ)–stability angle for other choices of the coefficients $\sigma_2 > 0$ and $\sigma_3 > 0$ satisfying (26). In this way, the reader can make different choices from ours, based on the desidered properties for the RKTASE3 method.

4.3 RK–TASE with Order Four

Here we consider a general RK–TASE method with four stages and order four, denoted with RKTASE4, that in view of (7)–(8) is obtained using the TASE operator $T_4(hW)$ defined by

$$T_4(z) = \frac{\pi_4(z) - z^4}{\pi_4(z)}, \quad \text{with} \quad \pi_4(z) = z^4 - \sigma_1\, z^3 + \sigma_2\, z^2 - \sigma_3\, z + \sigma_4.$$

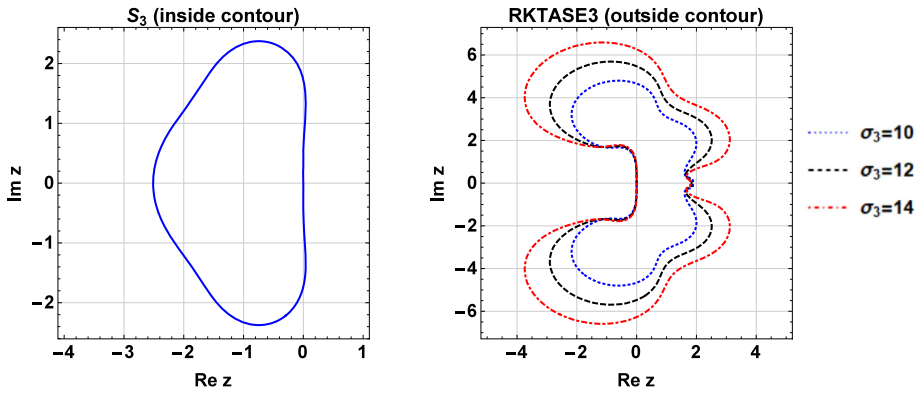

Fig. 3 On the left, region $\mathcal{S}_3$ (28); on the right, stability region of the RKTASE3 method with $\sigma_1 = 1.59607$, $\sigma_2 = \sigma_3/\sigma_1 + \epsilon$, $\epsilon = 10^{-5}$, and several values of σ_3.

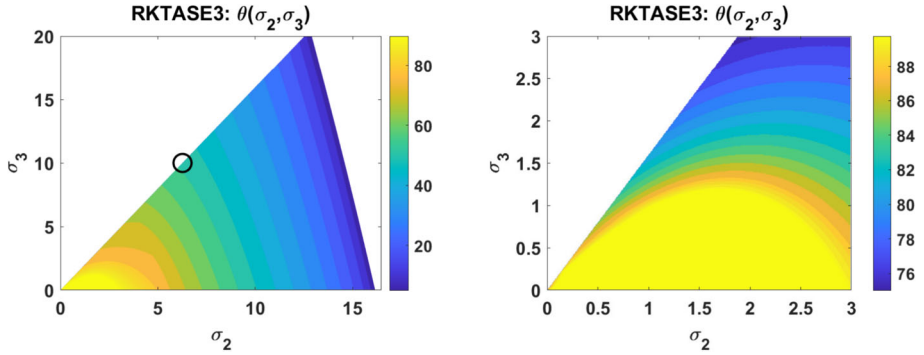

Fig. 4 Angle θ of L(θ)–stability ($\sigma_1 = 1.59607$) for RKTASE3, by varying σ_2 and σ_3 (zoom near the origin on the right); the symbol 'o' denotes the choice (σ_2, σ_3)=(6.26539, 10) that we made to conduct the numerical tests.

Using (19) from Theorem 1, we consider for stability the following conditions on the real coefficients σ_j:

$$\sigma_1 > 0,\ \sigma_2 > 0,\ \sigma_3 > 0,\ \sigma_4 > 0, \quad \text{and} \quad \sigma_1\sigma_2\sigma_3 - \sigma_3^2 - \sigma_1^2\sigma_4 > 0. \tag{30}$$

From (17), the stability function of the RKTASE4 method is

$$RT_4(z) = 1 + (z\ T_4(z)) + \frac{1}{2}\ (z\ T_4(z))^2 + \frac{1}{6}\ (z\ T_4(z))^3 + \frac{1}{24}\ (z\ T_4(z))^4\,; \tag{31}$$

also, the stability function of the underlying explicit RK is $R_4(z)$, corresponding to RT_4 with $T_4(z) = 1$, see (15).

Similarly to previous subsections, by Proposition 1 we take $-\sigma_1 \in \mathcal{S}_4$, which is shown in the left Figure 5. Recall from (16) that

$$\mathcal{S}_4 = \{z \in \mathbb{C} :\ |R_4(z)| \le 1\}. \tag{32}$$

The condition $-\sigma_1 \in \mathcal{S}_4$ leads to

$$\sigma_1 \in (0, z_4], \quad z_4 \simeq 2.78529.$$

Let us consider the following result.

Proposition 5 *The function* $|RT_4(\infty)|$ *attains its minimum value of* 0.270395 *at* $\sigma_1 \simeq 1.59607$, *for every* $\sigma_2,\ \sigma_3,\ \sigma_4$.

Proof From (18) and (31),

$$RT_4(\infty) = 1 - \sigma_1 + \frac{1}{2}\,\sigma_1^2 - \frac{1}{6}\,\sigma_1^3 + \frac{1}{24}\,\sigma_1^4.$$

By the positivity of $RT_4(\infty)$, it holds $|RT_4(\infty)| = RT_4(\infty)$. Its derivative with respect to σ_1 vanishes at $\sigma_1 \simeq 1.59607$, which is the minimum point for $RT_4(\infty)$.

Therefore, we consider the choice $\sigma_1 = 1.59607$. Moreover, to satisfy (30) we take

$$\sigma_2 = \frac{\sigma_3^2 + \sigma_1^2\sigma_4}{\sigma_1\sigma_3} + \epsilon, \quad \epsilon > 0. \tag{33}$$

From now on, we consider $\epsilon = 10^{-5}$, which yields values of σ_2 close to the smallest admissible ones satisfying the stability condition. This choice allows to reduce the propagation of round–off errors in the computation of $\pi_4(hW)$, since from (7)–(8), when $p = 4$, note that σ_2 scales the powers of hW, where W approximates the Jacobian of the problem. Then, we fix the two remaining free parameters σ_3 and σ_4 to obtain a good balance between the minimum error constant $|C_4| = 1/\sigma_4$ and a sufficiently large angle θ of strong A(θ)–stability. In [1] the authors derive RK–TASE methods with $\theta \simeq 88$ degrees but with error constant $C_4 \simeq 11$, see also the next Table 1. Here, we derive general RK–TASE methods with much smaller error constant. In particular, in numerical experiments, we consider the RKTASE4 method with $\sigma_3 = 2.8$ and $\sigma_4 = 16$, which is strongly A(θ)–stable with $\theta = 52.0013$ degrees and error constant $|C_4| = 1/\sigma_4 = 0.0625$. The right Figure 5 reports the stability region of this method.

Several numerical explorations that we performed by varying σ_2, σ_3 and σ_4 show that it is possible to obtain even lower error constants. However, this would imply a smaller stability region. To confirm this, we report in Figure 6 the strong A(θ)–stability angle for several values of $\sigma_4 > 0$, by varying $\sigma_2 > 0$ and $\sigma_3 > 0$.

4.4 RK–TASE with Order Greater than or Equal to Four

In this subsection we consider a general RK–TASE method with five stages, denoted with RKTASE5, that by (7)–(8) is obtained using the TASE operator $T_5(hW)$ below:

$$T_5(z) = \frac{\pi_5(z) - z^5}{\pi_5(z)}, \quad \text{with} \quad \pi_5(z) = z^5 - \sigma_1 z^4 + \sigma_2 z^3 - \sigma_3 z^2 + \sigma_4 z - \sigma_5. \tag{34}$$

We emphasize that so far in the scientific literature, RK–TASE methods with more than four stages and order $p \geq 4$ have not yet been proposed.

It is known that it is not possible to determine the coefficients of the underlying explicit RK method in such a way as to obtain order $p = 5$ (to do this, we need at least six stages), see e.g. [4]. Furthermore, the stability function of the underlying explicit RK method is not of type (15), and hence the stability function of the general RK–TASE method is not of type (17).

To study stability using similar strategies to those adopted so far, we then prove the following result. From now on, we take $c = Ae$, with $A,\ e$ as in (13), ensuring the same

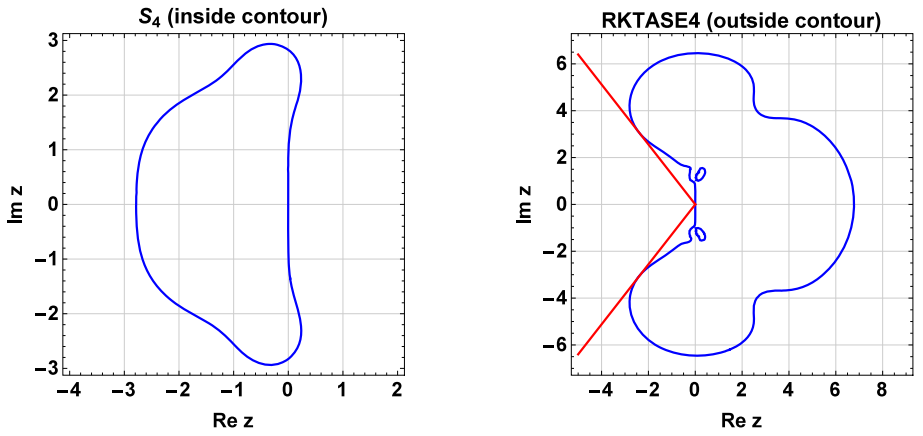

Fig. 5 On the left, region $\mathcal{S}_4$ (32); on the right, stability region of the RKTASE4 method with $\sigma_1 = 1.59607$, σ_2 as in (33) with $\epsilon = 10^{-5}$, $\sigma_3 = 2.8$ and $\sigma_4 = 16$, that is strongly A(θ)–stable with $\theta = 52.0013$ degrees.

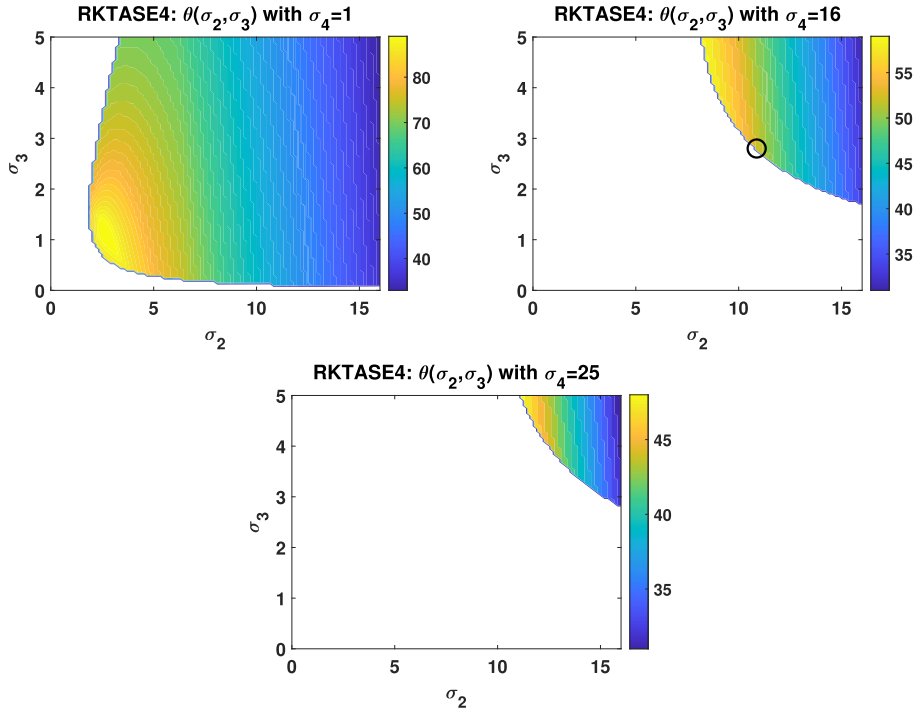

Fig. 6 Angle θ of strong A(θ)–stability ($\sigma_1 = 1.59607$) for RKTASE4, by varying σ_2 and σ_3, setting $\sigma_4 = 1, 16, 25$, respectively; the symbol 'o' in the plot corresponding to $\sigma_4 = 16$ denotes the choice of (σ_2, σ_3) that we made to conduct the numerical tests.

order for RK methods on autonomous and non–autonomous problems. We can then assume that f in (1) is in autonomous form.

Theorem 3 *Consider the RKTASE5 method where the underlying explicit RK method has order $p = 5$ on linear problems. Necessary conditions for the A–stability of RKTASE5 are the following:*

$$\sigma_j > 0, \quad j = 1, \dots, 5, \tag{35}$$
$$\sigma_1\sigma_2 - \sigma_3 > 0, \tag{36}$$
$$\sigma_1\sigma_2\sigma_3 + \sigma_1\sigma_5 - \sigma_3^2 - \sigma_1^2\sigma_4 > 0, \tag{37}$$
$$\sigma_4(\sigma_1\sigma_2\sigma_3 - \sigma_3^2 - \sigma_1^2\sigma_4) + \sigma_5(2\sigma_1\sigma_4 + \sigma_2\sigma_3 - \sigma_1\sigma_2^2 - \sigma_5) > 0. \tag{38}$$

Moreover,

$$\sigma_1 \in (0, z_5], \quad z_5 \simeq 3.21705, \tag{39}$$

is necessary for A(θ)–stability for any θ.

Proof For a 5–stage explicit RK method, using formula (12), one can easily verify that the stability function R is of the form

$$R(z) = 1 + (b^T\ e)\ z + (b^T\ c)\ z^2 + (b^T\ A\ c)\ z^3 + (b^T\ A^2\ c)\ z^4 + (b^T\ A^3\ c)\ z^5, \tag{40}$$

being $b,\ A,\ e$ as in (13) and $c = Ae$. By hypothesis, the RK method has order $p = 5$ on linear problems. Note that, if f in (1) is linear, i.e. $y' = Wy + g$ being $W \in \mathbb{R}^{d\times d}$ and $g \in \mathbb{R}^d$ constants, then all its derivatives with respect to y of order strictly greater than one are zero, and therefore in the Taylor expansion of the exact and numerical solution many elementary differentials do not appear. Actually, in the linear case the only elementary differentials which survive for order $p = 5$ are $f,\ f'f,\ f'f'f,\ f'f'f'f,\ f'f'f'f'f$, see [4, Table 310(II)]. The order conditions associated with these elementary differentials are

$$b^T\ e = 1, \quad b^T\ c = \frac{1}{2}, \quad b^T\ A\ c = \frac{1}{6}, \quad b^T\ A^2\ c = \frac{1}{24}, \quad b^T\ A^3\ c = \frac{1}{120}, \tag{41}$$

see [4, Tables 300(I), 310(II), 312(II) and Th. 315A]. Therefore, the stability function (40) corresponds exactly to $R_5 = R_5(z)$ in (15). It follows that the stability function of the RKTASE5 method is RT_5 in (17).

We can thus exploit a similar approach to the one used to prove Theorem 1: necessary conditions for A–stability are obtained by imposing the Routh–Hurwitz criterion on the polynomial $\pi_5(-z)$ in (34). This leads to (35), (36), (37), (38).

The last condition (39) follows from the fact that, since from the hypotheses of this theorem R is of the form (15) with $p = 5$, see (40)–(41), we can exploit Proposition 1. Hence, a necessary condition for A(θ)–stability is $-\sigma_1 \in \mathcal{S}_5$, where from (16)

$$\mathcal{S}_5 = \{z \in \mathbb{C} :\ |R_5(z)| \le 1\}. \tag{42}$$

$\mathcal{S}_5$ is represented in Figure 7. Recalling that $\sigma_1 \in \mathbb{R}$, $-\sigma_1 \in \mathcal{S}_5$ if and only if (39) holds. Thus, (39) is necessary for A(θ)–stability.

From now on in this subsection, let us consider the assumptions of Theorem 3 for the RKTASE5 method. In view of Remark 2, we will consider all the conditions of Theorem 3 in the search for A(θ)–stable methods.

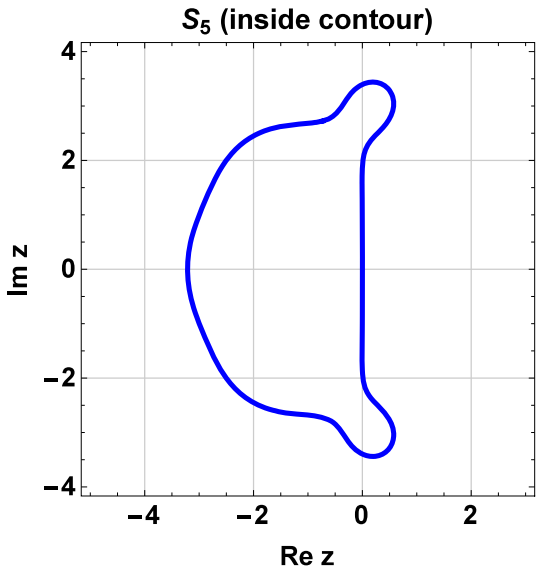

Fig. 7 Region $\mathcal{S}_5$ (42).

Remark 3 With five stages ($s = 5$), it is possible to construct an explicit RK method with order $p = 4$ for any problem and order $p = 5$ for linear problems. Consequently, it is possible to do the same for RKTASE5 thanks to (4). Actually, we emphasize that it is possible to reach order $p = 5$ even for some classes of nonlinear problems. For example, with $s = 5$ it is possible to impose order $p = 5$ for quadratic differential equations, where f in (1) is of the form

$$^k f(y) = \sum_{i=1}^{d} \sum_{j=1}^{i} {}^k w_{ij}\ {}^i y\ {}^j y + \sum_{i=1}^{d} {}^k v_i + {}^k \omega, \quad k = 1, \ldots, d,$$

denoting the left upper index the individual components of the associated vector, and being ${}^k w_{ij}, {}^k v_i, {}^k \omega$ some constants. In the numerical tests we use two different underlying explicit 5–stage RK methods, depending on the problem to be solved: for quadratic problems, we will consider a method of order $p = 5$; for general problems, we will consider a method of order $p = 4$, but still with $p = 5$ in the linear case in view of Theorem 3. In the Appendix, we report the related Butcher tableau and explain their derivation, which has been done by minimizing the respective error coefficients.

To fix the coefficients σ_j of the TASE operator, in addition to Theorem 3 we consider the following result.

Proposition 6 *The function* $|RT_5(\infty)|$ *attains its minimum value of* 0 *at* $\sigma_1 \simeq 2.18061$, *for every* $\sigma_2,\ \sigma_3,\ \sigma_4,\ \sigma_5$.

Proof From Theorem 3, the stability function of RKTASE5 is

$$RT_5(z) = 1 + (z\ T_5(z)) + \frac{1}{2}\ (z\ T_5(z))^2 + \frac{1}{6}\ (z\ T_5(z))^3 + \frac{1}{24}\ (z\ T_5(z))^4 + \frac{1}{120}\ (z\ T_5(z))^5\,.$$

Also, from (18),

$$RT_5(\infty) = 1 - \sigma_1 + \frac{1}{2}\,\sigma_1^2 - \frac{1}{6}\,\sigma_1^3 + \frac{1}{24}\,\sigma_1^4 - \frac{1}{120}\,\sigma_1^5.$$

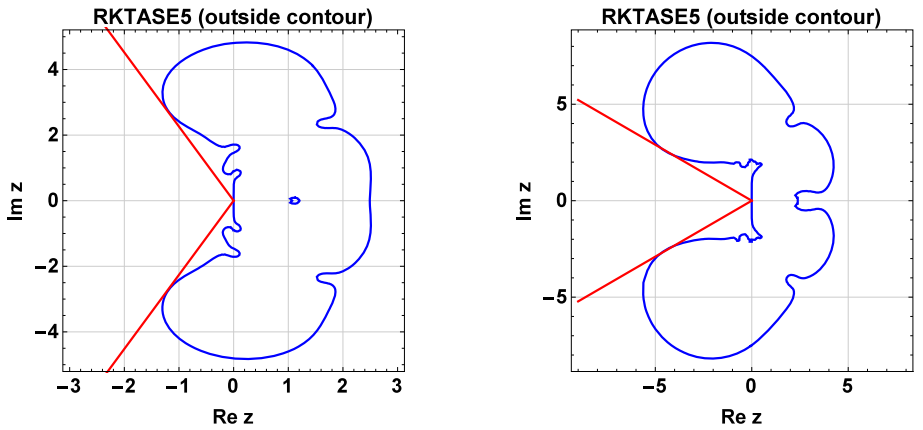

Fig. 8 On the left, stability region of RKTASE5 with $\sigma_1 = 2.18061$, $\sigma_2 = 8$, $\sigma_3 = 8$, $\sigma_4 = 6$, $\sigma_5 = 5$, that is L(θ)–stable with $\theta = 66.1317$; on the right, stability region of RKTASE5 with $\sigma_1 = 2.18061$, $\sigma_2 = 14.9843$, $\sigma_3 = 32.4926$, $\sigma_4 = 55.6196$, $\sigma_5 = 120$, that is L(θ)–stable with $\theta = 30.1137$ degrees.

Note that the equation $|RT_5(\infty)| = 0$ admits the real solution $\sigma_1 \simeq 2.18061$, from which the result follows.

In view of L(θ)–stability, we then fix $\sigma_1 = 2.18061$. Also, recall that the error constant of the TASE operator is $|C_5| = 1/\sigma_5$. Therefore, the goal is to make σ_5 as large as possible, obtaining simultaneously L(θ)–stability for some relatively high $\theta > 0$. To this aim, we performed two numerical explorations on the parameters σ_j, $j = 2, 3, 4, 5$: one to obtain a method with $\theta > 60$ degrees; one also allowing lower values of θ, but requiring $|C_5| < 10^{-2}$. In particular, the mentioned numerical explorations have been done by considering the conditions in Theorem 3 and the requirement

$$|RT_5(z)| \leq 1, \quad z \in \mathbb{R}, \quad z \leq 0,$$

which has been analyzed via a Moebius transformation from the interval $(-\infty, 0]$ to $(-1, 0]$. We thus got two RKTASE5 methods with the following coefficients:

$$\sigma_1 = 2.18061, \quad \sigma_2 = 8, \quad \sigma_3 = 8, \quad \sigma_4 = 6, \quad \sigma_5 = 5;$$
$$\sigma_1 = 2.18061, \quad \sigma_2 = 14.9843, \quad \sigma_3 = 32.4926, \quad \sigma_4 = 55.6196, \quad \sigma_5 = 120.$$

These methods are L(θ)–stable with $\theta = 66.1317$ and $\theta = 30.1137$ degrees, and have error coefficients $|C_5| = 0.2$ and $|C_5| = 0.0083$, respectively. Their stability regions are presented in Figure 8. In numerical experiments, we will use the latter.

4.5 Summary of the Obtained Results

In Table 1, we summarize the properties of the general RK–TASE methods derived in this paper, comparing them with those of the existing RK–TASE methods from the literature recalled in Section 2. In particular, in the table we have considered the following methods.

- **RKTs**: the extension of the original RK–TASE (RKT) methods [3] proposed in [9] of order $p = s = 2, 3, 4$.
- **RKTCs**: the RK–TASE methods with Complex (RKTC) coefficients proposed in [1] of order $p = s = 2, 3, 4$.

Table 1 Properties of RK–TASE methods, where p denotes the order of consistency, $|RT_p(\infty)|$ denotes $|\lim_{z\to\infty} RT_p(z)|$ being $RT_p(z)$ the stability function, θ denotes the A(θ)–stability angle, $|C_p|$ denotes the size of the error constant of the TASE operator.

Method	p	Stability	$\lvert RT_p(\infty)\rvert$	θ	$\lvert C_p\rvert$
RKT2				90	4.5
RKTC2	2	Strong A-stabiliy	0.5	90	0.5948
GRKT2				60.3955	0.2
RKT3				89.02	6.8838
RKTC3	3	L(θ)-stability	0	89.86	6.6406
GRKT3				50.4281	0.1
RKT4				87.34	44.3176
RKTC4	4	Strong A(θ)-stability	0.27	88.26	10.7996
GRKT4				52.0013	0.0625
GRKT5	4 or 5*	L(θ)-stability	0	66.1317	0.2
				30.1137	0.0083

*GRKT5 has order $p = 4$ in general, but reaches order $p = 5$ on quadratic problems.

- **GRKTs**: the new General RK–TASE (GRKT) methods proposed in this paper, of order $p = s = 2, 3, 4$, and with $s = 5$ and $p \geq 4$.

Note that the new GRKT5 is the only method that can reach order $p = 5$. All existing RK–TASE methods in the literature can instead reach at most order $p = 4$.

Remark 4 Table 1 shows that the new GRKTs methods are characterized by much lower error constants than those of existing RK–TASE methods, and still have quite large A(θ)–stability angles. Actually, for reaction–diffusion PDEs even smaller values of θ can be sufficient to perform the numerical integration without stability issues. Indeed, once space discretized with e.g. classical finite differences, these problems usually have a Jacobian with stiff part characterized by spectrum around the negative real axis.

In any case, as we will see from numerical experiments, the choice of methods with quite large θ can allow to efficiently treat even problems where the advection term is present. Furthermore, we emphasize that in this paper we have provided the stability properties of GRKTs methods also for coefficient values different from those considered by us (see Figures 2, 4 and 6). This can allow the user to choose the GRKTs method with the desired stability properties, based on the problem to be solved.

5 Numerical Experiments

This section is devoted to numerical experiments. As explained in the paper and summarized in Remark 4, the new general RK–TASE methods have been designed to be able to solve very efficiently reaction–diffusion problems, but also to handle possible advection terms. Therefore, we will consider experiments on reaction–diffusion PDEs, and also on a problem where an advection term is present. As we will see, the new GRKTs methods are a marked improvement over the existing RK–TASE methods, and are also very competitive with some exponential and splitting schemes.

In particular, we compare the new GRKTs schemes with the methods listed in Subsection 4.5, see also Table 1, and with the following ones.

- **SRKTs**: the Singly RK–TASE (SRKT) methods proposed in [7] of order $p = s = 2, 3, 4$.
- **STRANG2**: a Strang splitting method of order $p = 2$, see [23, p. 329].
- **ETDp**: the Exponential Time Differencing (ETD) methods of order $p = 2, 3, 4$, see e.g. [27].

The properties of RKTs and RKTCs, and the reasons behind their derivation, have been recalled in Section 2 and Subsection 4.5. SRKTs methods have similar errors and stability properties as RKTs, but they were designed to require the solution of linear systems (they foresee the solution of s^2 systems at each step to reach order $p = s$) always involving the same coefficient matrix, at each time–step. Finally, the Strang splitting and ETDp methods were designed to solve semi–linear problems $y'(t) = \mathcal{D}y(t) + g(t, y(t))$ accurately and stably, exploiting the so–called exponential φ–functions. In particular: STRANG2 integrates the linear part by two applications of $\varphi_0(\frac{h}{2}\mathcal{D}) = e^{\frac{h}{2}\mathcal{D}}$, and the nonlinear part by the two–stage order–two explicit midpoint RK; the ETDp schemes involve in their formulation exponential functions $\varphi_i(\frac{h}{2}\mathcal{D})$ and/or $\varphi_i(h\mathcal{D})$, $i \geq 0$, that can be defined iteratively as

$$\varphi_i(z) = \frac{\varphi_{i-1}(z) - \varphi_{i-1}(0)}{z}, \qquad \varphi_0(z) = e^z,$$

see [22, Eq. (2.11)].

For all the used TASE methods of order $p = s \leq 4$, the underlying explicit RK schemes are those reported in [3, Appendix A]. Regarding GRKT5, the employed methods are reported in the Appendix below. The RKTs, RKTCs and GRKTs methods are implemented using formulation (7)–(8) of the TASE operator (see also the Appendix), which improves their efficiency as observed in Remark 1. As for the SRKTs methods, we exploited the algorithm described in [7, p. 15]. All the RK–TASE methods are linearly implicit, and for them the linear systems to be solved have coefficient matrices involving $W \approx D_y(t, y)$ in their expression. Regarding the STRANG2 and ETDp methods, details on their implementation are reported in the remark below.

Remark 5 The performance of the STRANG2 and ETDp methods depends heavily on the strategy used to compute the φ–functions. Therefore, we examined several alternatives:

- calculating a–priori (before the numerical integration) the Taylor series of $\varphi_i(\frac{h}{2}\mathcal{D})$ and/or $\varphi_i(h\mathcal{D})$, $i \geq 0$, as reported in [27, Eqs. (A.5)–(A.6)]; in this case, the series was truncated after M_* terms, being
$$M_* = c_* \, e_N \, h \, \max(\mathrm{eig}(\mathcal{D})),$$
according to [27, Eq. (A.7)], where c_* (> 1) represents a "safety factor" to be fixed for stability reasons, and e_N, h, $\mathcal{D}$ denote respectively the Napier number, the step–size, the linear part of the problem;
- calculating a–priori (before the numerical integration) the functions $\varphi_i(\frac{h}{2}\mathcal{D})$ and/or $\varphi_i(h\mathcal{D})$, $i \geq 0$, through the solution of some underlying integral equations by means of quadrature formulas; for this purpose, we used the MATLAB code `phiquad`[1] from [5, 6];
- evaluating the action of $\varphi_i(\frac{h}{2}\mathcal{D})$ and/or $\varphi_i(h\mathcal{D})$, $i \geq 0$, on vectors; for this purpose, we used the MATLAB code `phisplit`[2] from [5, 6].

In the implementation, we employed the second approach, since it turned out to be the most efficient for the semi–linear problems considered in the numerical tests below.

[1] https://github.com/caliarim/phisplit/blob/main/phiquad.m.

[2] https://github.com/caliarim/phisplit/blob/main/phisplit.m.

At this stage, it is worth emphasizing the ease of implementation of the GRKTs methods (see the Appendix); in fact, the RK–TASE methods were introduced to allow users without expertise in advanced numerical techniques to efficiently solve stiff differential problems.

Numerical tests have been performed using a computer with processor Intel(R) Core(TM) i7–10700 CPU 2.90 GHz, RAM of 16 Gb, Windows 11 Pro 64–bit 24H2, and the version R2024b of MATLAB. We have exploited built–in tools such as the `lu` function (see also the Appendix below) and, when appropriate, the `sparse` format for matrix storage. For each of the PDEs problems considered in the experiments, we have computed a reference solution of the related semi–discretized version with the MATLAB built–in function `ode15s`, setting $\texttt{AbsTol} = \texttt{RelTol} = 10^{-14}$. This reference solution has then been used to determine the errors of the methods, calculated at the end point of the time grid, and the estimated order of convergence, as

$$\frac{\log(\text{error}(2h)) - \log(\text{error}(h))}{\log(2)}.$$

Here and below, error(h) denotes the absolute error in infinity norm provided by the method, at the last grid point of the time interval of the semi–discretized problem solved using step–size h.

5.1 Burgers Equation

Let us consider the Burgers equation in the form

$$\frac{\partial u}{\partial t} = \epsilon \frac{\partial^2 u}{\partial x^2} - \frac{1}{2}\frac{\partial u^2}{\partial x}, \qquad (x,t) \in [0, 2\pi] \times (0,1], \quad \epsilon = \frac{1}{100},$$

equipped with periodic boundary conditions and initial condition

$$u(x, t_0) = \begin{cases} 1, & x \in [0, \pi], \\ 0, & x \in (\pi, 2\pi), \end{cases}$$

similarly to [9, Subsec. 3.2]. We perform a spatial discretization with finite differences of order four for both the diffusion and advection terms. The resulting system of the form (1) $y'(t) = f(t, y(t))$ with initial condition $y(t_0) = y_0$ reads

$$y'(t) = \epsilon \mathcal{D} y(t) - \frac{1}{2}\mathcal{P} y(t)^2, \quad y \in \mathbb{R}^d, \quad \mathcal{P},\ \mathcal{D} \in \mathbb{R}^{d\times d},$$

being $\mathcal{P}$ and $\mathcal{D}$ the discretization matrices associated with the first and second order derivatives, respectively. We consider $d = 2^7$, and $W = D_y f(t_0, y_0)$ for all the methods used in the experiments. That is, in accordance with Remark 1 we select constant W corresponding to the Jacobian at the initial point. Since the semi–discretized problem is quadratic, for GRKT5 we use as underlying scheme the method reported in Subsection 8.1, in the Appendix below, so as to achieve order $p = 5$.

The results are reported in Figure 9 and Table 2. Figure 9 reports the CPU time in seconds and the corresponding absolute error in infinity norm computed at the last grid point for all the considered methods of order $p = 2, 3$ and $p \geq 4$, respectively, for $h = (t_{\text{end}} - t_0)/2^N$, $N = 5, \ldots, 13$. Table 2 reports, for several values of h, error(h) and the estimated order of convergence by the general RK–TASE methods.

The results show that the GRKTs methods are more efficient than the RKTs, RKTCs and SRKTs methods, for $s = 2, 3, 4$. That is: GRKT2 method reaches 10 times smaller errors than RKT2 and SRKT2, and slightly smaller errors than RKTC2, at the same computational

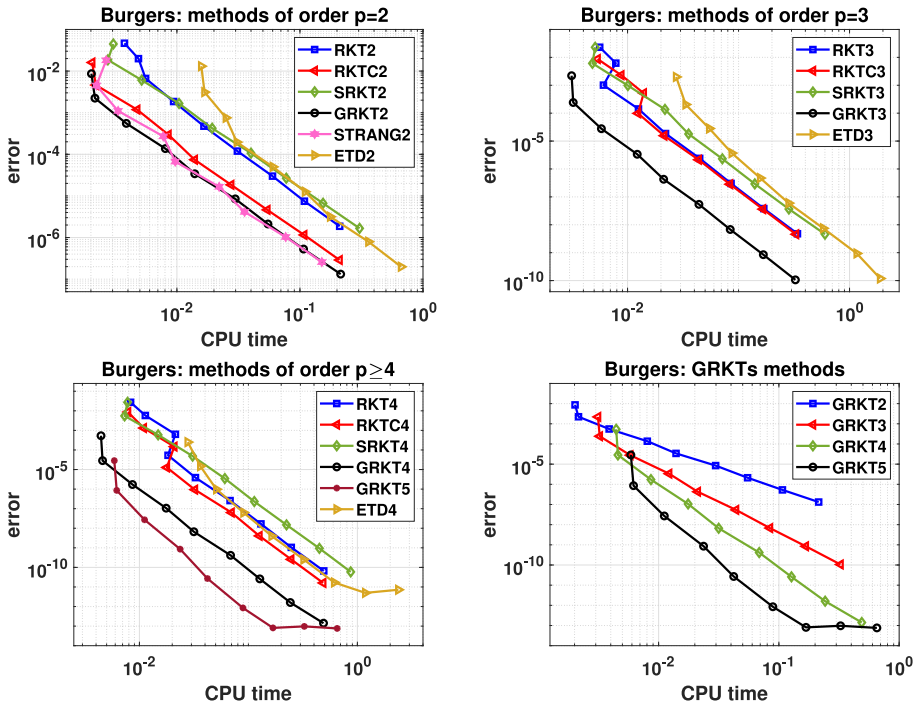

Fig. 9 Efficiency plots of the methods used with step–size $h = (t_{\text{end}} - t_0)/2^N$, $N = 5, \ldots, 13$, on the Burgers equation; the last one compares the GRKTs schemes all together.

cost; GRKT3 achieves 10 times smaller errors than all other considered TASE methods of order $p = s = 3$; finally, the GRKT4 method reaches 100 times smaller errors than all other considered TASE methods of order $p = s = 4$. Furthermore, note from Table 2 that the GRKT5 method exhibits order $p = 5$, in accordance with the fact that the semi–discretized problem is quadratic. Therefore, as clearly visible from Figure 9, in this case the use of GRKT5 is very convenient, as it achieves errors even 1000 times smaller than the other RK–TASE methods with similar computational cost. Regarding the comparison with the ETDp methods, $p = 2, 3, 4$, note that the GRKTs schemes of the same order exhibit very similar errors, but take less computing times, thus being more efficient. STRANG2, on the other hand, is extremely competitive with GRKT2. To conclude, note that the RKTs and RKTCs methods, for $s = 3, 4$, show a jump in the efficiency plots in Figure 9 at some large values of the step–size h. This behavior seems typical of these methods, as also visible in [1, Figs. 7–8], but in any case it occurs only for relatively large step–sizes, where small fluctuations of the CPU times are to be expected. Even in the numerical tests of the next subsections, the RKTs and RKTCs methods show such behavior.

5.2 A Vegetation Model

Let us consider a reaction–diffusion model for vegetation growth in arid environments, introduced in [15] and consisting of a system of three PDEs describing the growth of two different

Table 2 Error and experimental order of convergence p of GRKTs methods used with step–size $h = (t_{\text{end}} - t_0)/2^N$, $N = 7, \ldots, 11$, on the Burgers equation.

	GRKT2		GRKT3		GRKT4		GRKT5	
N	Error	p	Error	p	Error	p	Error	p
7	2.23e-03	-	2.41e-04	-	2.85e-05	-	8.59e-07	-
8	5.53e-04	2.01	2.78e-05	3.12	1.72e-06	4.05	2.70e-08	4.99
9	1.37e-04	2.01	3.37e-06	3.04	1.06e-07	4.01	8.57e-10	4.98
10	3.41e-05	2.01	4.28e-07	2.97	6.63e-09	4.00	2.70e-11	4.99
11	8.48e-06	2.01	5.40e-08	2.99	4.14e-10	4.00	8.51e-13	4.99

tree species u_1 and u_2 as the available water w varies:

$$\begin{cases} \dfrac{\partial u_1}{\partial t} = \dfrac{\partial^2 u_1}{\partial x^2} + w u_1(u_1 + H u_2) - B_1 u_1 - S u_1 u_2, \\ \dfrac{\partial u_2}{\partial t} = D\dfrac{\partial^2 u_2}{\partial x^2} + F w u_2(u_1 + H u_2) - B_2 u_2, \qquad x \in [x_0, x_{\text{end}}],\ t > t_0 = 0. \\ \dfrac{\partial w}{\partial t} = d\dfrac{\partial^2 w}{\partial x^2} + A - w - w(u_1 + u_2)(u_1 + H u_2), \end{cases} \tag{43}$$

This model has the coexistence of the two plants as a metastable solution, as proved in [15]. That is, for relatively short time intervals, the coexistence of u_1 and u_2 can be observed. However, over long time intervals, one of the two species disappears. Therefore, to observe this property it is necessary to employ methods that are stable for long time integrations. Also in [14] the authors considered (43) to test the efficiency of a class of two–step peer methods preconditioned with TASE operators.

Let us take the following values of the parameters: $A = 1.5$, $B_1 = 0.45$, $B_2 = 0.3611$, $F = 0.802$, $H = 0.802$, $S = 0.0002$, $d = 500$, $D = 0.802$. We take the initial conditions $u_1(x, t_0) = u_2(x, t_0) = w(x, t_0) = 1+\cos(x)$, and periodic boundary conditions. The spatial discretization is performed with finite differences of order two. The resulting system of the form (1) is of type $y'(t) = \mathcal{D}y(t) + g(t, y(t))$, being $\mathcal{D} \in \mathbb{R}^d$, $d = 3m$, a tridiagonal block matrix with the coefficients of the discretization of the diffusion terms. We consider $W = \mathcal{D}$ for all the methods used in the experiments. That is, in accordance with Remark 1 we select constant W corresponding to the Jacobian of the diffusion part, which is the one responsible for the stiffness of the problem. Since the semi–discretized problem is not quadratic, in this case for GRKT5 we use the method reported in Subsection 8.2, in the Appendix below, as the underlying scheme, so as to have a very small error constant.

First of all, we apply the methods taking $t \in (t_0, t_{\text{end}}]$, $t_{\text{end}} = 1$, $x_0 = -50$, $x_{\text{end}} = 50$, and $m = 2^6$, with step–size $h = (t_{\text{end}} - t_0)/2^N$, $N = 6, \ldots, 14$. The related results, reported in Figure 10 and in Table 3, are similar to those obtained in the previous subsection and once again testify the better efficiency of the new GRKTs over all the other considered schemes. Note that, although GRKT5 now has order four, due to its extremely low error constant it still provides significantly smaller errors than all other TASE methods with $p = 4$, as visible in Table 3 and Figure 10. Thus, since its computational cost is comparable to that of the other RK–TASE methods of the same order, the use of GRKT5 can be advantageous in this case too. Furthermore, note that, unlike the previous case, ETDp methods now provide in general smaller errors than GRKTs schemes of the same order. However, the lower computing times

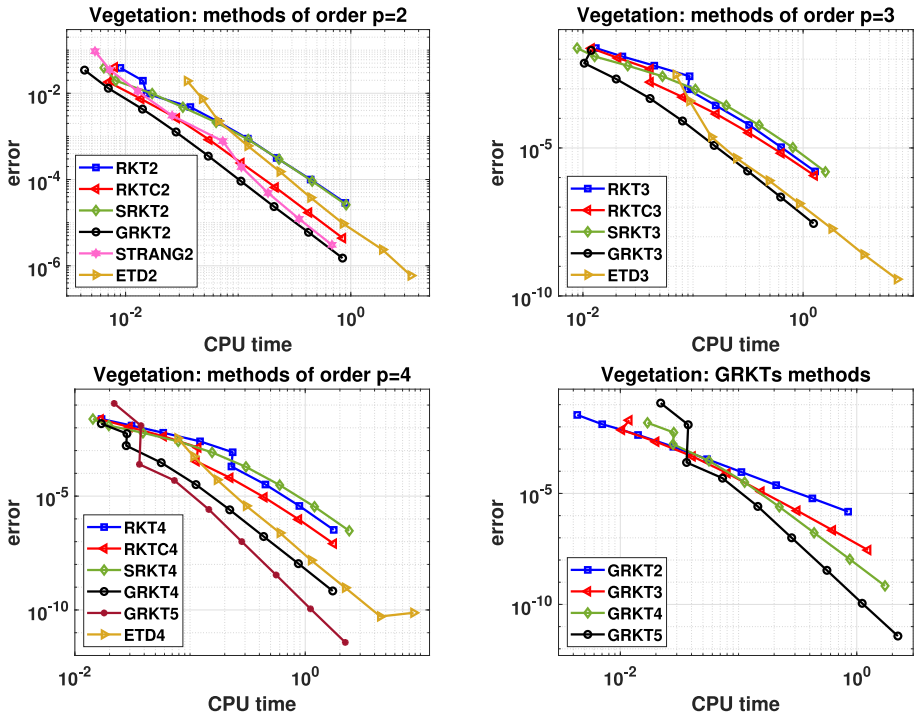

Fig. 10 Efficiency plots of the methods used with step–size $h = (t_{\text{end}} - t_0)/2^N$, $N = 6, \ldots, 14$, on the vegetation model; the last one compares the GRKTs schemes all together.

Table 3 Error and experimental order of convergence p of GRKTs methods used with step–size $h = (t_{\text{end}} - t_0)/2^N$, $N = 10, \ldots, 14$, on the vegetation model.

	GRKT2		GRKT3		GRKT4		GRKT5	
N	Error	p	Error	p	Error	p	Error	p
10	3.49e-04	-	8.15e-05	-	3.20e-05	-	2.60e-06	-
11	9.18e-05	1.92	1.22e-05	2.74	2.50e-06	3.68	1.00e-07	4.69
12	2.36e-05	1.96	1.67e-06	2.87	1.68e-07	3.89	3.43e-09	4.87
13	5.99e-06	1.98	2.19e-07	2.93	1.08e-08	3.96	1.12e-10	4.94
14	1.51e-06	1.99	2.81e-08	2.97	6.83e-10	3.98	3.76e-12	4.90

of the latter still make GRKTs more efficient. Observe also that GRKT2 performs better than STRANG2.

Finally, Figure 11 reports the numerical solution u_1 provided by the GRKTs methods on the vegetation model (43), selecting $m = 2^7$, $t_{\text{end}} = 1500$ and $h = (t_{\text{end}} - t_0)/2^{17} \approx 1.14 \cdot 10^{-2}$. In agreement with [15], with the considered values of the parameters and by selecting this spatial interval, for u_1 the formation of non–homogeneous vegetation patterns initially occurs. Then, over long times the quantity of biomass u_1 tends to progressively decrease. Note, from Figure 11, that all the GRKTs methods are able to reproduce this trend. Therefore, they are stable and reliable even for long time integrations.

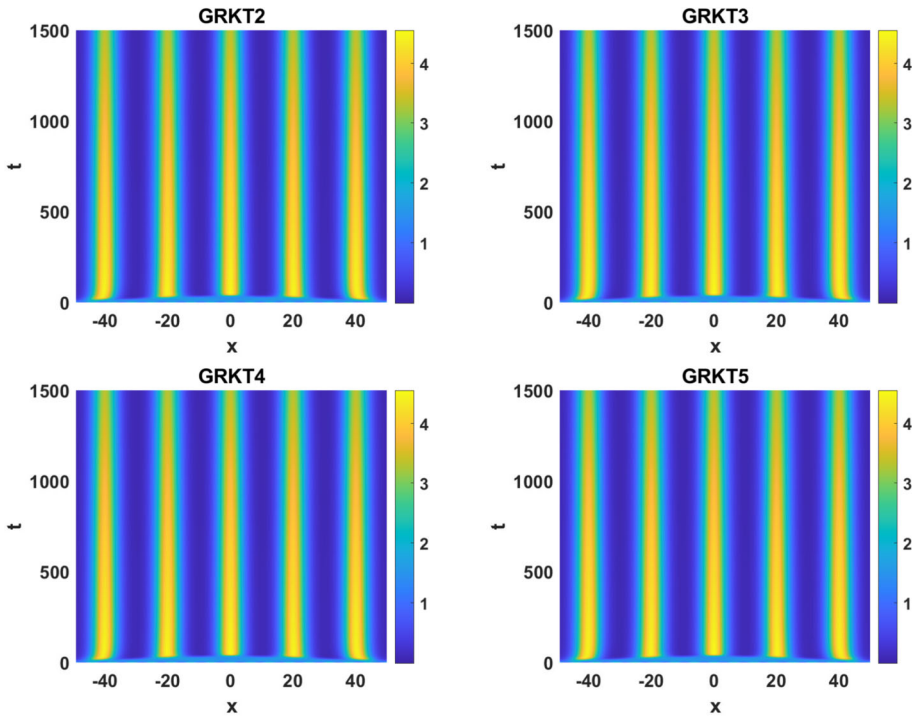

Fig. 11 Component u_1 of the solution of the vegetation model (43) provided by GRKTs methods.

5.3 DIB Model

Finally, we consider the DIB model [17, 18], that has been introduced to describe the electrodeposition process in batteries. For certain parameter choices, the model shows Turing pattern–like solutions in agreement with experimental observations conducted on batteries. Therefore, for this model the availability of efficient solvers is very important, as it requires integration over long time intervals. In particular, the DIB is a 2D reaction–diffusion model of the form

$$\begin{cases} \dfrac{\partial \eta}{\partial t} = \Delta \eta + \rho f_1, \quad f_1 = A_1(1-\theta)\eta - A_2\eta^3 - B(\theta - \alpha), \\ \dfrac{\partial \theta}{\partial t} = d\Delta\theta + \rho f_2, \quad f_2 = C(1+k_2\eta)(1-\theta)(1-\gamma(1-\theta)) - D\theta(1+\gamma\theta)(1+k_3\eta), \end{cases}$$

see [17, Sec. 5], where $\eta : \Omega \times (0, t_{\text{end}}] \to \mathbb{R}$ and $\theta : \Omega \times (0, t_{\text{end}}] \to [0, 1]$. We take $\Omega = [0, 15]^2$, zero Neumann boundary conditions, and initial condition

$$\eta(x_1, x_2, t_0) = 10^{-5}\ \texttt{rand}(x_1, x_2), \quad \theta(x_1, x_2, t_0) = \alpha + 10^{-5}\ \texttt{rand}(x_1, x_2),$$

being `rand` the MATLAB function that generates uniformly distributed random numbers. The considered parameters are $\alpha = 0.5, \gamma = 0.2, \rho = 1, A_1 = 10, A_2 = 30, B = 66, C = 3, d = 20, D = 2.4545, k_2 = 2.5, k_3 = 1.5$. We perform the spatial discretization through the same number of points in both directions x_1 and x_2, with finite differences of order two using the ghost points strategy, see e.g. [23], to impose the zero Neumann boundary conditions. The semi–discretized problem reads $y'(t) = \mathcal{D}y(t) + g(t, y(t))$, $\mathcal{D} \in \mathbb{R}^d$, $d = 2m^2$, being $\mathcal{D}$

Table 4 Error and experimental order of convergence p of GRKTs methods used with step–size $h = (t_{\text{end}} - t_0)/2^N$, $N = 5, \ldots, 9$, on the DIB model.

	GRKT2		GRKT3		GRKT4		GRKT5	
N	Error	p	Error	p	Error	p	Error	p
5	1.68e-06	-	5.40e-07	-	3.28e-07	-	5.72e-08	-
6	4.33e-07	1.95	8.89e-08	2.60	3.55e-08	3.21	2.78e-09	4.36
7	1.10e-07	1.97	1.33e-08	2.74	2.72e-09	3.71	1.04e-10	4.75
8	2.78e-08	1.99	1.82e-09	2.87	1.82e-10	3.90	3.44e-12	4.91
9	7.00e-09	1.99	2.39e-10	2.93	1.16e-11	3.97	1.54e-13	4.48

a block tridiagonal matrix; its blocks are of the type $I \otimes \mathcal{A} + \mathcal{A} \otimes I$, being I the identity and $\mathcal{A} \in \mathbb{R}^m$ the matrix with the discretization coefficients of the second order derivatives. We consider $m = 16$, and $W = \mathcal{D}$ similarly to the vegetation model of the previous subsection. Since the semi–discretized problem is not quadratic, for GRKT5 we use as underlying scheme the method reported in Subsection 8.2, in the Appendix.

Figure 12 and Table 4 allow to evaluate, in analogy to the previous subsections, the performance of all the considered methods and the experimental order of convergence of the GRKTs schemes, respectively. They were obtained by applying the methods for $t \in (t_0, t_{\text{end}}]$, $t_0 = 0$, $t_{\text{end}} = 1$, and $h = (t_{\text{end}} - t_0)/2^N$, $N = 4, \ldots, 11$. Also in this case, we observe the better efficiency of GRKTs methods compared to the other considered RK–TASE schemes, and the advantage of GRKT5 compared to the other methods of the same order. Indeed, GRKT5 shows order $p = 4$, but its low error constant allows to obtain better results than the other methods. Finally, GRKTs methods have important efficiency advantages over ETDp schemes. Furthermore, note that GRKT2 is more efficient than STRANG2 for large step–sizes, while as h decreases the latter shows reduced computation times (thus, for a stable solution in short times, the first is preferable). This behaviour arises because, here, reducing the step–size does not substantially increase the cost of computing the involved φ–functions.

Finally, to evaluate the reliability of the methods for high values of h over large time intervals, even as the size of the semi–discretized problem increases, we solved the DIB taking $m = 31$ (thus the size of the semi–discretized problem is almost $2 \cdot 10^3$), in the interval $(t_0, t_{\text{end}}] = (0, 50]$, with $h = (t_{\text{end}} - t_0)/2^9 \approx 0.1$ for the schemes of order two, and $h = (t_{\text{end}} - t_0)/2^8 \approx 0.2$ for the other schemes. The results are summarized in Figure 13, where we plot the η solution at the final time obtained with all the RK–TASE methods considered in the experiments, and the reference solution. As can be observed, the GRKTs methods are the only ones that accurately reproduce the trend of the reference solution. This is very important, as an unreliable solution may not allow accurate predictions about the type of patterns to expect. Thus, even in this case the new GRKTs methods are advantageous.

6 Conclusions

In this paper we have derived new methods belonging to the family of RK–TASE methods by exploiting a formulation of the TASE operator that allows to improve their efficiency. We analyzed the accuracy and stability properties of the new general RK–TASE methods, and this allowed to select the related coefficients to get particularly performing numerical schemes of order $p = 2, 3, 4$ for the efficient solution of reaction–diffusion PDEs. Furthermore, we

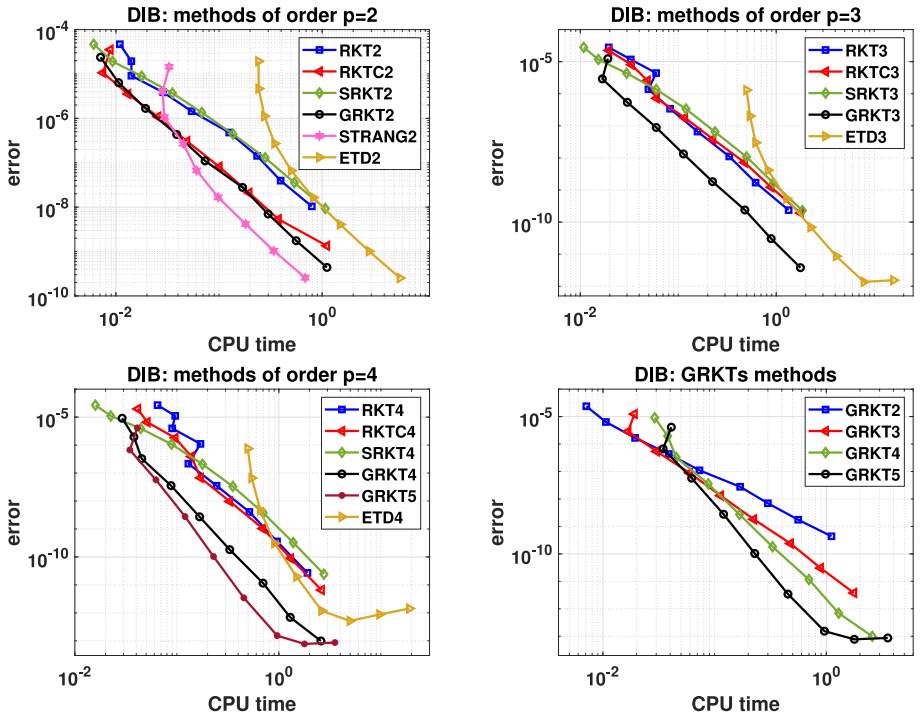

Fig. 12 Efficiency plots of the methods used with step–size $h = (t_{\text{end}} - t_0)/2^N$, $N = 4, \ldots, 11$, on the DIB model; the last one compares the GRKTs schemes all together.

have proposed 5–stage RK–TASE methods that can reach order $p = 5$ for several problems. We emphasize that this is the first paper where RK–TASE methods of order greater than four are proposed.

Several numerical experiments performed on reaction–diffusion systems of PDEs from applications, in both 1 and 2 spatial dimensions, and also on an advection–diffusion PDE, have confirmed the theoretical analysis and shown the efficiency of the new RK–TASE methods, which are stable and much more accurate than existing RK–TASE methods at the same computational cost. Moreover, they showed that the new RK–TASE methods are competitive/advantageous with respect to ETD schemes and a Strang splitting scheme.

An interesting research activity that can be carried out from this paper lies in the theoretical study of the stability of general RK–TASE methods with inexact Jacobian, analogously to what was done in [12] for the RK–TASE methods introduced in [9]. Furthermore, future developments could concern a revisitation of GRKTs methods for the efficient solution of semi–discretized PDEs defined in a large number of spatial dimensions, following the approach used e.g. in [11] for a class of W–methods.

7 Appendix A: Implementation and Computational Cost of General RK–TASE Methods

Here, we report the pseudocode for the implementation of the general RK–TASE methods, see Algorithm 1, and analyze their computational cost. For simplicity of presentation, and

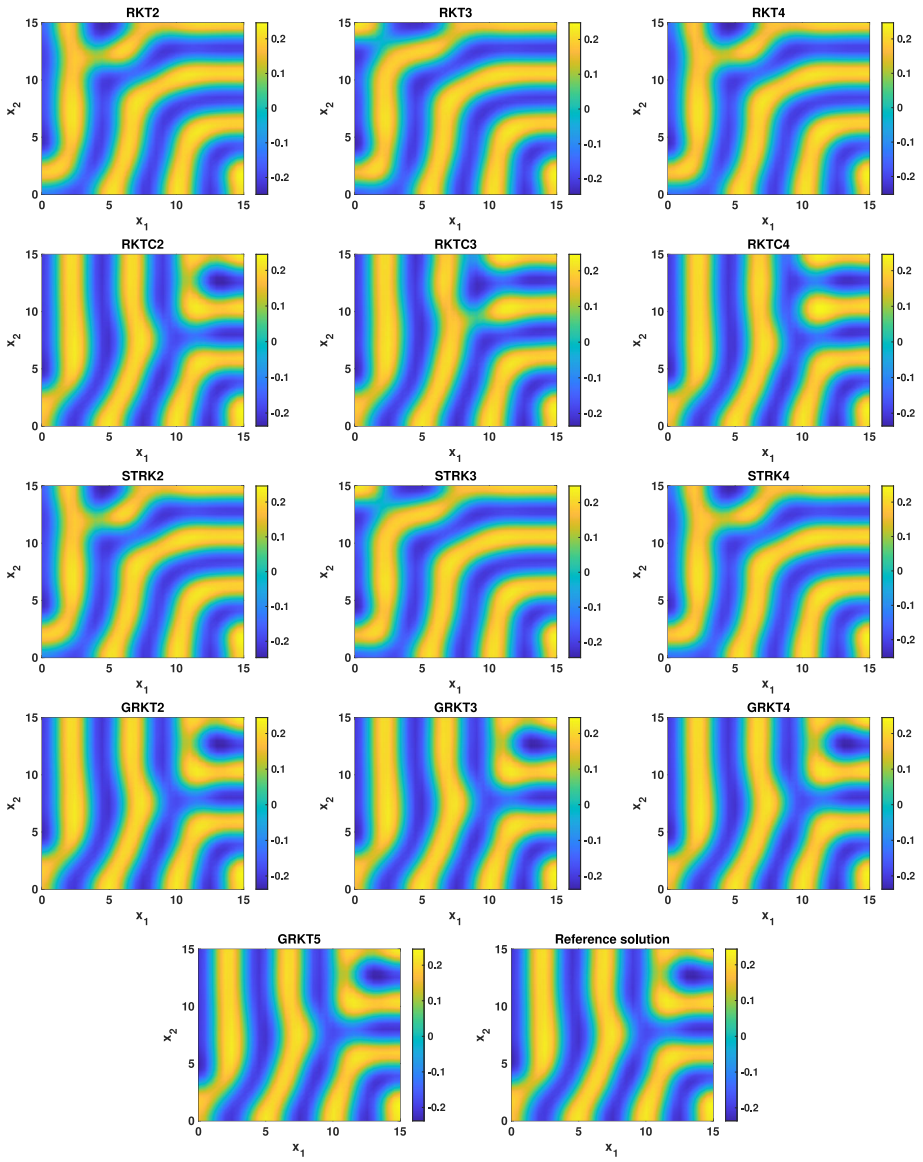

Fig. 13 Component η of the solution of the DIB model at time $t = 50$ provided by the RKTs (first row), RKTCs (second row), SRKTs (third row), GRKTs (fourth and fifth row), and `ode15s` (fifth row at the end).

since this is also the case considered in the numerical experiments, we assume that the matrix W of size $d \times d$ involved in the formulation of the TASE operator is constant throughout the numerical integration. In the following: we denote by N the number of subintervals into which the domain $[t_0, t_{\text{end}}]$ is partitioned for the time integration; we denote $f_i = f(t_0 + c_i h, y_0 + \sum_{j=1}^{i-1} a_{ij} K_j)$; we mention the MATLAB functions `lu` for computing the LU factorization of a matrix and `backslash` for solving linear systems.

Algorithm 1 Pseudocode for implementing the general RK–TASE methods

1: compute $\pi_{p-1}(hW) = -\sigma_1(hW)^{p-1} + \sigma_2(hW)^{p-2} + \ldots + (-1)^p\sigma_p$
2: compute $\pi_p(hW)$ as in (8); it is $\pi_{p-1}(hW) + (hW)^p$
3: compute $[L, U] = \text{lu}\,(\pi_p(hW))$
4: **for** $n = 2, \ldots, N+1$ **do**
5: **for** $i = 1, \ldots, s$ **do**
6: compute $\hat{f}_i = h\,\pi_{p-1}(hW)\,f_i$
7: compute $K_i = U\backslash(L\backslash\hat{f}_i)$
8: **end for**
9: compute $y_n = y_{n-1} + \sum_{j=1}^{s} b_j K_j$
10: **end for**

From Algorithm 1, note that the main computational cost of the general RK–TASE methods is given by the following operations:

- calculation of $p-1$ matrix products needed to determine $\pi_{p-1}(hW)$ and $\pi_p(hW)$ in rows 1, 2;
- calculation of the LU factorization of $\pi_p(hW)$ in row 3;
- calculation of s matrix–vector products at each step, see line 6;
- solution of $2s$ triangular linear systems at each step, see line 7.

Taking advantage of the analysis performed in [1, Sec. 4], the computational cost is therefore given by

$$\mathcal{O}\left(3\,s\,N\,d^2 + \frac{3p-2}{3}\,d^3\right).$$

To conclude, it is worth mentioning that, for reasons of numerical stability, in some cases in the implementation it may be preferable to use the Horner algorithm both for the computation of π_{p-1} and π_p, and for performing the matrix–vector products in line 6.

8 Appendix B: Underlying Explicit RK Methods of Order $p = 4, 5$

The RK order conditions and their connections to the elementary differentials and Butcher trees can be found e.g. in [4, Tables 300(I), 310(II), 312(II) and Th. 315A]. Exploiting them, here we describe the derivation of the two underlying explicit RK methods that we used for RKTASE5. First of all, to fix the coefficients of both methods, we considered the conditions

$$c = Ae, \qquad b^T A = b^T - (b * c)^T,$$

denoting '$*$' the component–wise product, and those in (41). Indeed, they allow to, respectively: get the same order on both autonomous and non–autonomous problems; significantly reduce the total number of order conditions; reach order $p = 5$ on linear problems, so that we can exploit the stability theory derived in Subsection 4.4.

8.1 Explicit RK of Order Five on Quadratic problems

First, together with the above conditions, we required the remaining ones to get order $p = 4$ on general problems. Then, to obtain a RK method of order $p = 5$ on quadratic problems, we considered only the related order conditions involving elementary differentials $f^{(m)}$ with

$m < 3$. Indeed, the others are zero on quadratic problems. In this way, we got a family of five stages, fifth order explicit RK methods depending on the three parameters c_2, c_3 and c_4, forced to satisfy the algebraic relation

$$\begin{aligned} g(c_2, c_3, c_4) = {} & 3(-2+5c_2)\big(-3(-1+c_4)(-4+5c_4) + c_2(9+5(-2+c_4)c_4)\big) + \\ & 5\big(-42 + 3c_2(31+3c_2) + 96c_4 - c_2(180+91c_2)c_4 + (6+c_2)\cdot \\ & (-9+20c_2)c_4^2\big)c_3 - 50\big(3 - 7c_4 + 4c_4^2 + 2c_2^2(-3+7c_4) + \\ & c_2(-3-6(-1+c_4)c_4)\big)c_3^2 = 0. \end{aligned}$$

Subsequently, we considered the vector LTE_5 containing the local truncation error constants, i.e.

$$\mathrm{LTE}_5 = \frac{1}{\sigma(\tau)}\Big(\Phi(\tau) - \frac{1}{\gamma(\tau)}\Big),$$

for any Butcher tree τ of order $\rho(\tau) = 6$ where no node has more than two children (since $f^{(m)}$ is zero for $m \geq 3$), with eleven non-zero components. The Butcher trees and the functions $\Phi(\tau)$, $\sigma(\tau)$, $\gamma(\tau)$, $\rho(\tau)$ are defined in [4, Ch. 3]. The parameters c_2, c_3, and c_4 were therefore finally set by computing

$$\begin{aligned} & \min_{c_2,\, c_3,\, c_4} ||\mathrm{LTE}_5||_2 \\ & \text{subject to } g(c_2, c_3, c_4) = 0, \text{ and } c_2, c_3, c_4 \in [0, 1]. \end{aligned}$$

That is, we minimized the 2-norm of the vector LTE_5, requiring order $p = 5$ on quadratic problems. This led to the method having the Butcher tableau reported below, for which $||\mathrm{LTE}_5||_2 = 2.19 \cdot 10^{-3}$. It belongs to the family of RK schemes proposed in [29].

$$\begin{array}{c|ccccc} 0 & & & & & \\ \frac{1}{4} & \frac{1}{4} & & & & \\ \frac{1}{2} & -\frac{1}{6} & \frac{2}{3} & & & \\ \frac{3}{5} & \frac{3}{250} & \frac{42}{125} & \frac{63}{250} & & \\ 1 & \frac{3}{10} & \frac{6}{35} & -\frac{9}{10} & \frac{10}{7} & \\ \hline & \frac{1}{9} & \frac{16}{63} & 0 & \frac{125}{252} & \frac{5}{36} \end{array}$$

8.2 Explicit RK of Order Four with Small Error Constant

We followed the procedure described in the first part above, before fixing c_2, c_3 and c_4. Indeed, as mentioned this allows to have order $p = 4$ on general problems, and also to annihilate some of the error terms associated with the elementary differentials that survive for quadratic problems. In this case, the local truncation error coefficients are the elements of the vector

$$\mathrm{LTE}_4 = \frac{1}{\sigma(\tau)}\Big(\Phi(\tau) - \frac{1}{\gamma(\tau)}\Big), \quad \forall\ \tau \text{ s.t. } \rho(\tau) = 5.$$

LTE_4 has nine components, of which six are zero in this case. The minimization of the related 2-norm led to $c_2 = 1/6$, $c_3 = (55 - \sqrt{19})/120$ and $c_4 = 5/6$. With this choice, $||\mathrm{LTE}_4||_2 = 1.99 \cdot 10^{-4}$. Below is the Butcher tableau of the obtained explicit RK method.

$$
\begin{array}{c|ccccc}
0 & & & & & \\
\frac{1}{6} & \frac{1}{6} & & & & \\
\frac{55-\sqrt{19}}{120} & -\frac{991}{4200}+\frac{\sqrt{19}}{42} & \frac{9(108-5\sqrt{19})}{1400} & & & \\
\frac{5}{6} & \frac{526621-15302\sqrt{19}}{321642} & \frac{-475019+2933\sqrt{19}}{193563} & \frac{280(190501+3743\sqrt{19})}{32325021} & & \\
1 & -\frac{8(196103+10871\sqrt{19})}{268035} & \frac{2740783+197771\sqrt{19}}{258084} & -\frac{280(181363604+19599553\sqrt{19})}{10807332021} & \frac{3(6233+441\sqrt{19})}{20060} & \\
\hline
 & \frac{1192+49\sqrt{19}}{15030} & \frac{697-49\sqrt{19}}{4020} & \frac{196000(153751+1420\sqrt{19})}{70803175203} & \frac{3(1807+49\sqrt{19})}{20060} & \frac{1082-49\sqrt{19}}{21030}
\end{array}
$$

Funding: Open access funding provided by Università degli Studi di Napoli Federico II within the CRUI-CARE Agreement. This work has been supported by GNCS–INdAM projects and by the Italian Ministry of University and Research (MUR), through the PRIN PNRR 2022 projects *BAT–MEN* (P20228C2PP, CUP: F53D23010020001) and *MatForPat* (P2022WC2ZZ, CUP: E53D23018030001). Also, this work has been partially supported by the Spanish Project PID2022–141385NB–I00 of Ministerio de Ciencia e Innovación.

Data Availability This paper has no associated data.

Declarations

Conflict of interest The authors declare that they have no conflict of interest.

References

1. Aceto, L., Conte, D., Pagano, G.: On a generalization of time-accurate and highly-stable explicit operators for stiff problems. Appl. Numer. Math. **200**, 2–17 (2024)
2. Aceto, L., Conte, D., Pagano, G.: Modified TASE Runge-Kutta methods for integrating stiff differential equations. SIAM J. Sci. Comput., **47**(3), (2025)
3. Bassenne, M., Fu, L., Mani, A.: Time-accurate and highly-stable explicit operators for stiff differential equations. *J. Comput. Phys.*, 424, (2021)
4. Butcher, J.C.: Numerical methods for ordinary differential equations, 2nd edn. John Wiley & Sons Ltd, Chichester (2008)
5. Caliari, M., Cassini, F.: Direction splitting of φ-functions in exponential integrators for d-dimensional problems in Kronecker form. *J. Approx. Softw.*, 1(1), (2024)
6. Caliari, M., Cassini, F.: A second order directional split exponential integrator for systems of advection–diffusion–reaction equations. *J. Comput. Phys.*, 498:112640, (2024)
7. Calvo, M., Fu, L., Montijano, J. I., Rández, L.: Singly TASE operators for the numerical solution of stiff differential equations by explicit Runge–Kutta schemes. *J. Sci. Comput.*, 96(1), (2023)
8. M. Calvo, S. González-Pinto, J. I. Montijano. Runge-Kutta methods for the numerical solution of stiff semilinear systems. *BIT Numer. Math.*, 40:611–639, (2000)
9. Calvo, M., Montijano, J. I., Rández, L.: A note on the stability of time–accurate and highly–stable explicit operators for stiff differential equations. *J. Comput. Phys.*, 436, (2021)
10. Calvo, M., Montijano, J. I., Rández, L.: Modified Singly-Runge–Kutta-TASE methods for the numerical solution of stiff differential equations. *J. Sci. Comput.*, 103(1), (2025)

11. Conte, D., González-Pinto, S., Hernández-Abreu, D., Pagano, G.: On Approximate Matrix Factorization and TASE W-methods for the Time Integration of Parabolic Partial Differential Equations. J. Sci. Comput. **100**(2), 34 (2024)
12. Conte, D., Martin-Vaquero, J., Pagano, G., Paternoster, B.: Stability theory of TASE–Runge–Kutta methods with inexact Jacobian. SIAM J. Sci. Comput. **46**, A3638–A3657 (2024)
13. Conte, D., Pagano, G., Paternoster, B.: Nonstandard finite differences numerical methods for a vegetation reaction–diffusion model. *J. Comput. Appl. Math.*, 419, (2023)
14. Conte, D., Pagano, G., Paternoster, B.: Time-accurate and highly-stable explicit peer methods for stiff differential problems. *Comm. Nonlinear Sci. Numer. Simul.*, 119, (2023)
15. Eigentler, L., Sherratt, J.A.: Metastability as a coexistence mechanism in a model for dryland vegetation patterns. Bull. Math. Biol. **81**, 2290–2322 (2019)
16. Frasca-Caccia, G., Valentino, C., Colace, F., Conte, D.: An overview of differential models for corrosion of cultural heritage artefacts. *Math. Model. Nat. Phenom.*, 18, (2023)
17. Frittelli, M., Sgura, I.: Matrix-oriented FEM formulation for reaction-diffusion PDEs on a large class of 2D domains. Appl. Numer. Math. **200**, 286–308 (2024)
18. Frittelli, M., Sgura, I., Bozzini, B.: Turing patterns in a 3D morpho-chemical bulk-surface reaction-diffusion system for battery modeling. Math. Eng. **6**(2), 363–393 (2024)
19. Gantmacher, F.R.: The theory of matrices. AMS Chelsea Publishing, Providence, RI, first edition (1998)
20. González-Pinto, S., Hernández-Abreu, D., Pagano, G., Pérez-Rodríguez, S.: Generalized TASE RK methods for stiff problems. Appl. Numer. Math. **188**, 129–145 (2023)
21. Hairer, E., Wanner, G.: *Solving ordinary differential equations II. Stiff and Differential-Algebraic Problems*. Springer Series in Computational Mathematics (14). Springer, Berlin, (1996)
22. Hochbruck, M., Ostermann, A.: Exponential integrators. Acta Numer., 19:209–286, (2010)
23. Hundsdorfer, W., Verwer, J.: *Numerical Solution of Time-Dependent Advection-Diffusion Reaction Equations*. Springer, (2007)
24. Karagiannis-Axypolitidis, N., Panebianco, F., Bonanomi, G., Giannino, F.: Plants' competition under autotoxicity effect: an evolutionary game. Optim. Lett. **18**, 855–872 (2024)
25. Lu, H., Tartakovsky, D.M.: Lagrangian dynamic mode decomposition for construction of reduced-order models of advection-dominated phenomena. J. Comput. Phys. **407**, 109229 (2020)
26. Pagano, G.: Stabilized explicit peer methods with parallelism across the stages for stiff problems. Appl. Numer. Math. **207**, 156–173 (2025)
27. Permyakova, E. V., Goldobin, D. S.: High-order schemes of exponential time differencing for stiff systems with nondiagonal linear part. *J. Comput. Phys.*, 510:113493, (2025)
28. Rosenbrock, H.H.: Some general implicit processes for the numerical solution of differential equations. Comput. J. **5**, 329–330 (1963)
29. Van Daele, M., Vanden Berghe, G., De Meyer, H.: Explicit fifth order Runge-Kutta methods with five stages for quadratic ODEs. *Numerical Analysis and Its Applications*, pages 528–535, (1997)